

TRANSIENT ANALYSIS OF LAYERED COMPOSITE PLATES ACCOUNTING
FOR TRANSVERSE SHEAR STRAINS AND VON KARMAN STRAINS

by

DANIEL JOSEPH MOOK

THESIS submitted to the Faculty of the
Virginia Polytechnic Institute and State University
in partial fulfillment of the requirements for the degree of
MASTER OF SCIENCE
in
ENGINEERING MECHANICS

APPROVED:

J. N. REDDY

DANIEL FREDERICK

WAYNE W. STINCHCOMB

June, 1982
Blacksburg, Virginia

ACKNOWLEDGEMENTS

Dr. J. N. Reddy, Professor ESM, Virginia Tech, made this work possible. His expert advice and encouragement were indispensable to the completion of this project, and will be forever appreciated. Dr. Reddy also provided a large part of the computer code used in the analysis, saving the author the typically frustrating task of debugging a large portion of the program.

I would also like to express my appreciation for the helpful comments of Dr. Daniel Frederick and Dr. Wayne Stinchcomb, and to thank them for serving on my thesis committee.

Karen Mook, wife of the beleaguered author, not only provided many conveniences during the harrowing ordeal, but also contributed several of the figures. In addition, she tediously served as a sounding board for many versions of the text which appears herein. My love goes with my respect and appreciation for her contributions.

It is a pleasure to acknowledge the skillful typing of the equations and the figure captions by Sharon Larkins, my friend and neighbor.

This work was predominantly funded by a research grant from the Structural Mechanics Section of the Air Force Office of Scientific Research (Grant AFOSR-81-0142). The support is gratefully acknowledged.

CONTENTS

ACKNOWLEDGEMENTS	ii
----------------------------	----

Chapter

page

I.	INTRODUCTION	1
	MOTIVATION	1
	BRIEF LITERATURE REVIEW	5
	CONTRIBUTION OF THIS THESIS	7
II.	GOVERNING EQUATIONS FOR A LAYERED ANISOTROPIC PLATE	8
	FORM OF DISPLACEMENT AND STRAIN FIELDS	8
	STRAIN - DISPLACEMENT EQUATIONS	11
	STRESS - STRAIN RELATIONS	12
	EQUATIONS OF MOTION	14
III.	DEVELOPMENT OF THE COMPUTER PROGRAM	18
	COMMENTS	18
	VARIATIONAL FORMULATION	18
	THE FINITE ELEMENT PROGRAM	21
	BRIEF OUTLINE OF THE FEM	21
	THE TIME-MARCHING SCHEME	22
	SPECIAL CONSIDERATIONS	26
IV.	VERIFICATION AND RESULTS	31
	COMMENTS	31
	VERIFICATION	31
	EFFECT OF ROTARY INERTIA AND TRANSVERSE SHEAR CONSTANT	37
	PARAMETRIC RESULTS	41
V.	SUMMARY AND CONCLUSIONS	50
	SUMMARY	50
	CONCLUSIONS	51
	REFERENCES	53

Appendix

	<i>page</i>
A. MASS AND STIFFNESS MATRICES IN PROGRAM	55
B. FLOW DIAGRAM OF COMPUTER PROGRAM	59
C. LISTING OF COMPUTER PROGRAM	62
VITA	85
ABSTRACT	

LIST OF FIGURES

<i>Figure</i>	<i>page</i>
1. Fiber-Reinforced Laminated Composite Plate	2
2. Shear Deformation In The x-z Plane	9
3. Stress Resultants and Surfaces of Integration	17
4. Effect Of On Stability Of Solution	24
5. Finite Element Mesh	27
6. Alternate Forms Of Boundary Conditions	29
7. Comparison Of Results Using Different Boundary Conditions .	30
8. Comparison With Classical and Analytical Linear Theory	32
9. Comparison With Linear Results From Akay	34
10. Comparison With Nonlinear Results From Akay	36
11. Effect of Transverse Shear Constant - A Specific Example . .	38
12. Effect of Rotary Inertia in a Specific Example	40
13. Effect of Load Magnitude	43
14. Effect of Orthotropy	44
15. Effect of Plate Aspect Ratio	45
16. Effect of Lamination Scheme	47
17. Effect of Plate Thickness	49

Chapter 1
INTRODUCTION

1.1 MOTIVATION

In recent years, use of composite-material structures has grown considerably. With their high stiffness-to-weight ratios, composite materials are especially attractive in applications where strength is required and light weight is desirable. Typically, such applications are in moving structures such as aircraft, where a reduction in the weight of the structure may lead to better performance and/or a higher payload. Moving structures are usually subjected to dynamic (time-dependent) loads, and so it is often necessary to perform transient analyses of composite plates.

Many of these composites are so-called 'fiber-reinforced laminates', consisting of layers of relatively high stiffness fibers imbedded in a relatively low-stiffness matrix which is essentially isotropic. Often, all fibers within a layer are oriented in the same direction, thereby producing a 'transversely isotropic' state of orthotropy in the layer. In the case of a laminated plate, the fibers are parallel to the midplane. The fiber directions of the layers may be arbitrarily oriented with respect to a set of global axes x, y in the plane of the plate (z normal to the plate), as shown in Figure (1). A plate composed of layers arbitrarily oriented to the global axes will, in general, exhibit anisotropic

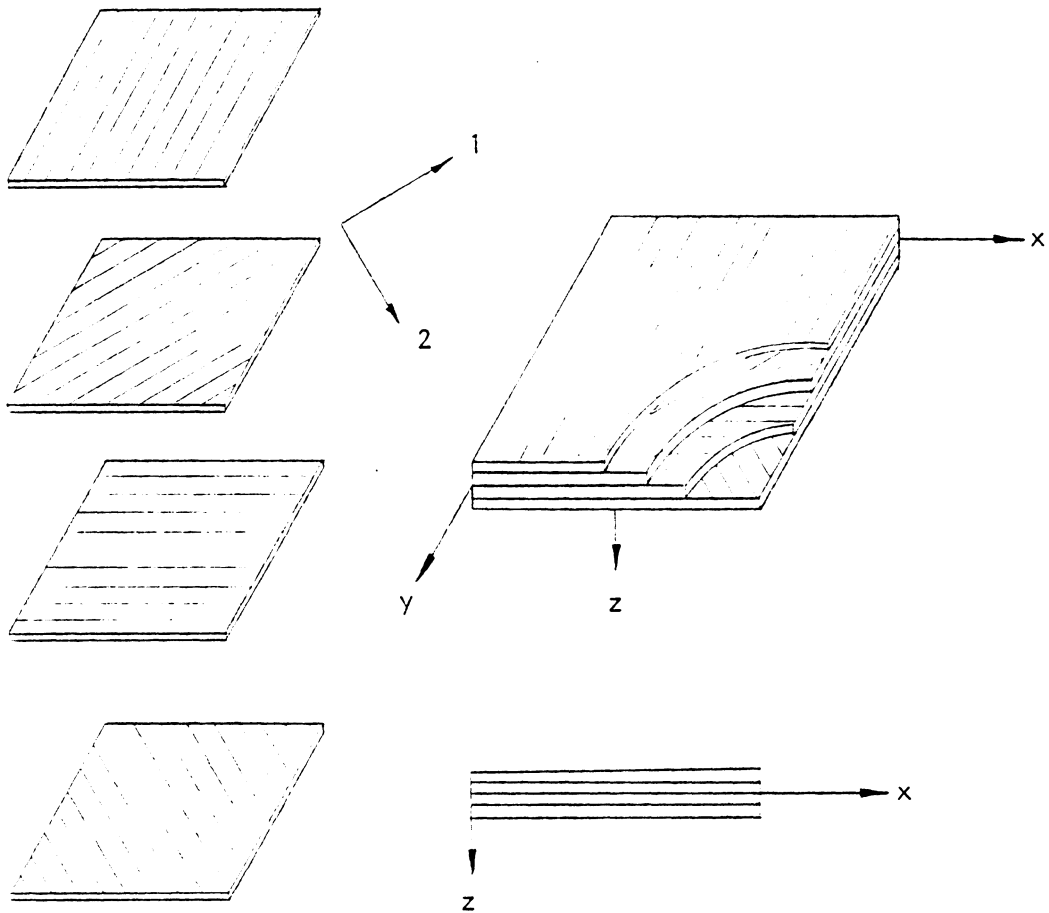


Figure 1 Fiber-Reinforced Laminated Composite Plate.

The straight lines represent fiber directions in the layer. In general, laminated plates are anisotropic with respect to axes (x, y, z) although each layer is transversely isotropic in the material principal coordinates $(1, 2, 3)$.

material properties. Thus, it is desirable to have an accurate, systematic, and efficient procedure to analyze the response of anisotropic laminated composite structures to dynamic loads.

Classical (Kirchhoff) thin-plate theory is frequently inadequate in predicting the response of laminated composite plates. For example, the classical theory assumes that normals to the undeformed midplane of the plate remain straight and normal to the midplane after deformation. This assumption implies that transverse shear deformation is negligible.

Fiber-reinforced composites typically exhibit high in-plane Young's moduli compared to the transverse shear modulus, so that transverse shear deformation is much more pronounced than in isotropic plates. This can be shown in the following manner. The stress-strain relations for transversely isotropic materials may be written

$$\begin{Bmatrix} \epsilon_1 \\ \epsilon_2 \\ \epsilon_3 \\ \gamma_{23} \\ \gamma_{31} \\ \gamma_{12} \end{Bmatrix} = \begin{bmatrix} S_{11} & S_{12} & S_{12} & 0 & 0 & 0 \\ & S_{22} & S_{23} & 0 & 0 & 0 \\ & & S_{22} & 0 & 0 & 0 \\ & & & 2(S_{22} - S_{23}) & 0 & 0 \\ & & & & S_{55} & 0 \\ & & & & & S_{55} \end{bmatrix} \begin{Bmatrix} \sigma_1 \\ \sigma_2 \\ \sigma_3 \\ \tau_{23} \\ \tau_{31} \\ \tau_{12} \end{Bmatrix} \quad (1.1.1)$$

where

$$\begin{aligned}
 S_{11} &= \frac{1}{E_{11}}, & S_{22} &= \frac{1}{E_{22}}, & S_{12} &= -\frac{\nu_{21}}{E_2}, & S_{23} &= \frac{-\nu_{32}}{E_3} = \frac{-\nu_{23}}{E_2}, \\
 S_{55} &= \frac{1}{G_{23}}
 \end{aligned} \quad (1.1.2)$$

Clearly, as the in-plane Young's moduli (E_1, E_2) increase relative to the transverse shear modulus G_{23} , the effects of transverse shear become more pronounced (i.e., S_{44} increases relative to the rest of the compliance matrix).

There is another problem which results from neglecting transverse shear strains. Transversely isotropic materials in general have 5 independent elastic constants, as shown in eqn (1.1.2). However, if the transverse shear strains γ_{23} and γ_{13} are neglected, then the elastic constant G_{23} does not enter into the analysis. Thus, a further effect of neglecting transverse shear strains is an inability to account for five independent constants in the analysis.

Therefore, in analyzing laminated composites, it is necessary to account for transverse shear deformation. In this thesis, a shear-deformable theory due to Yang, Norris, and Stavsky (1) is employed to predict the bending of laminated composite plates. The mathematical details are explained in Chapter II.

Furthermore, classical plate theory assumes that the transverse deflection is small compared to the thickness of the plate. When the transverse deflection is not small compared to the thickness, there is coupling between the membrane (in-plane) stresses and the curvatures. This coupling takes the form of 'midplane stretching'; i.e., the large curvatures stretch the midplane, introducing strains which, in turn, cause stresses. Large deflection adds nonlinear terms to the equations of motion, which are developed in Chapter II. These effects are often

referred to in the literature as 'geometric nonlinearities'. In this paper, the well-known von Karman assumptions are used to account for geometric nonlinearities. Essentially, these assumptions include the derivatives of the transverse displacement and their products, but ignore products of the derivatives of the in-plane displacements.

1.2 *BRIEF LITERATURE REVIEW*

Numerous authors have proposed shear deformation theories in the literature. In this review, only those works which contributed to the theory used herein are included. The intent is to trace the development of this theory from the earliest and simplest cases to the present analysis.

In 1945, Reissner (2) investigated the effect of transverse shear deformation in the bending of isotropic plates. Mindlin (3) investigated the effects of rotatory inertia and transverse shear deformation on the flexural motions of isotropic elastic plates. The so-called Reissner-Mindlin theory, although limited to isotropic plates, forms the basis for the laminated anisotropic plate theory.

The first treatment of shear deformation in a laminated plate is apparently due to Stavsky (4), who considered only isotropic layers with identical Poisson's ratios. Ambartsumyan (5) developed a theory for symmetric laminated plates whose layers are orthotropic. However, the material principal axes of each layer had to coincide with the plate coordinate axes (i.e., symmetric cross-ply).

The most general theory for arbitrarily laminated plates composed of anisotropic layers is due to Yang, Norris, and Stavsky (1). Their theory is an extension of the Reissner-Mindlin theory for homogeneous isotropic plates. Several writers have verified that the YNS theory is accurate in predicting transverse deflections and natural frequencies of laminated anisotropic plates. The YNS theory is incorporated in this work.

Pryor and Barker (6) are credited with the first finite-element analysis of a layered composite plate. Their work included transverse shear but not geometric nonlinearities. Numerous other writers have performed finite-element analyses including either transverse shear deformation or geometric nonlinearities, but not both.

Noor and Hartley (7) accounted for transverse shear deformation while finding approximate solutions to the large-deflection theory (in the von Karman sense) of laminated composite plates. However, the element they developed is algebraically complex and involves numerous degrees-of-freedom per node, and is neither practical nor efficient for general analysis work.

Reddy (8) developed a penalty (i.e., C^0) plate-bending element for laminated composite plate analysis. This element accounted for transverse shear deformation, and was simple and efficient to implement. Reddy and Chao (9) extended the element for the nonlinear bending analysis of laminated composite plates. Reddy and Mook (10) extended the nonlinear capability to the transient analysis of laminated

composite plates. This thesis includes the work presented therein, plus some additional analysis carried out using the same technique.

1.3 *CONTRIBUTION OF THIS WORK*

Apparently, this work represents the first finite-element analysis of the transient response of laminated composite plates which accounts for both transverse shear deformation and geometric nonlinearities (in the von Karman sense).

The finite element method (FEM) is employed to find the displacement at any particular time, using the variational principle of minimum potential (strain) energy. The Newmark direct integration technique is used to integrate the governing equations in time. Comparisons with previously reported results for simple linear and nonlinear cases (including 'exact' solutions) indicate that the method is accurate. The method is then used to investigate the parametric effects of various plate properties such as thickness, lamination scheme, load magnitude, and others.

Chapter II

GOVERNING EQUATIONS FOR A LAYERED ANISOTROPIC PLATE

2.1 FORM OF DISPLACEMENT AND STRAIN FIELDS

As in classical plate theory, the in-plane displacements are assumed to be at most linear variables through the thickness of the plate. Note that this requires the layers to be perfectly bonded so that the displacements are continuous through the thickness. The transverse displacement is assumed constant through the thickness (i.e., there is no transverse normal strain). Note that this assumes the shear strains to be small so that $\cos \gamma_{xz} = 1$. Thus, we may have both shearing strains and a constant transverse deflection simultaneously (see Figure 2).

With these assumptions, the displacement field is assumed to be of the form

$$\begin{aligned} u(x,y,z,t) &= u^0(x,y,t) + z\psi_x(x,y,t) \\ v(x,y,z,t) &= v^0(x,y,t) + z\psi_y(x,y,t) \end{aligned} \quad (2.1.1)$$

$$w(x,y,z,t) = w^0(x,y,t)$$

where u, v are the in-plane displacements; ψ_x, ψ_y are the rotations about the y and x axes, respectively, of a straight line normal to the midplane in the undeformed state; w is the transverse displacement; and u^0, v^0, w^0 are the displacements of the reference surface (i.e., $z=0$).

Similarly, the strains are of the form

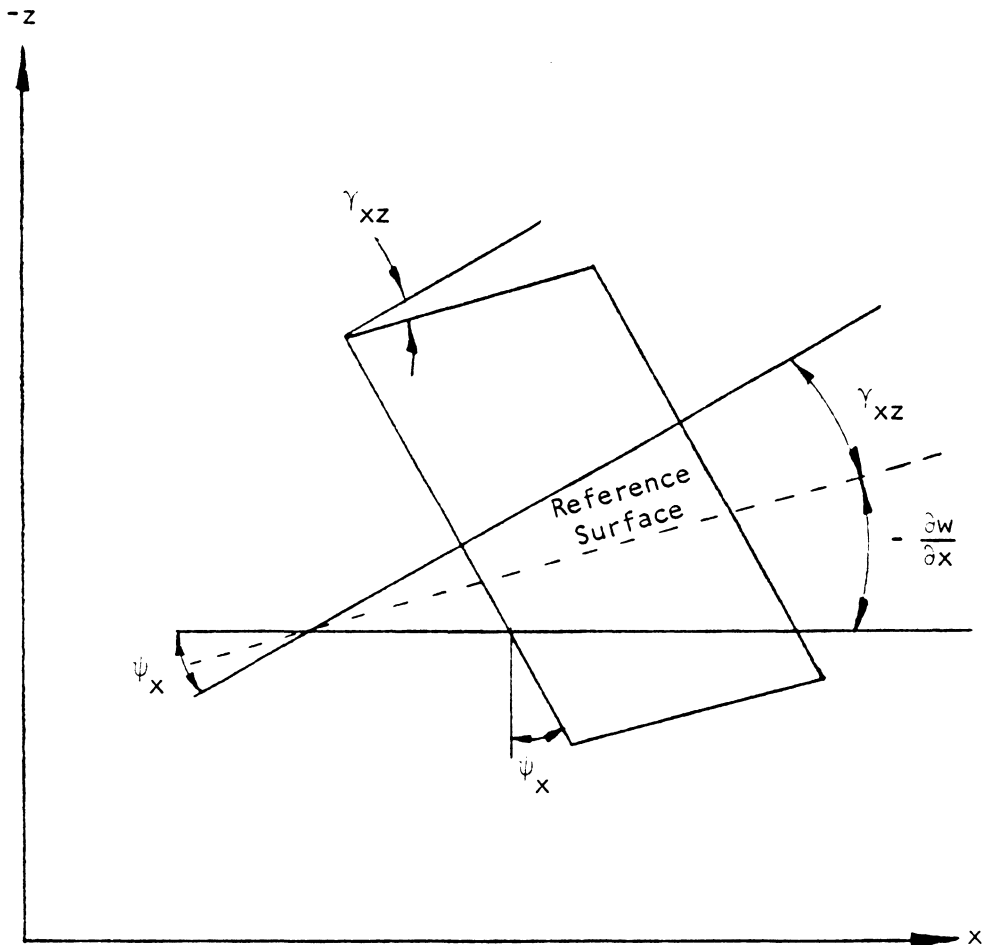


Figure 2 Shear Deformation in the x-z Plane.

γ_{xz} = shear deformation

$-\frac{\partial w}{\partial x}$ = slope of the reference surface

$\psi_x = \gamma_{xz} = -\frac{\partial w}{\partial x}$ = total rotation

$$(\varepsilon_x, \varepsilon_y, \gamma_{xy}) = (\varepsilon_x^0, \varepsilon_y^0, \gamma_{xy}^0) + z(\kappa_x, \kappa_y, \kappa_{xy}), \quad \varepsilon_z = 0 \quad (\text{assumed}) \quad (2.1.1)$$

where $\kappa_x, \kappa_y, \kappa_{xy}$ are the curvatures of the reference surface and are given by

$$\kappa_x = \psi_{x,x} \quad \kappa_y = \psi_{y,y} \quad \kappa_{xy} = \psi_{x,y} + \psi_{y,x} \quad (2.1.3)$$

The transverse shear strains are of the form (see Fig. 2)

$$\gamma_{xz} = w_{,x}^0 + \psi_x \quad (2.1.4)$$

$$\gamma_{yz} = w_{,y}^0 + \psi_y$$

Rearranging, the rotations are

$$\psi_x = -w_{,x}^0 + \gamma_{xz} \quad (2.1.5)$$

$$\psi_y = -w_{,y}^0 + \gamma_{yz}$$

and now the addition of transverse shear is clear. In classical plate theory the transverse shear terms are ignored, giving

$$\psi_x^c = -w_{,x}^0 \quad \psi_y^c = -w_{,y}^0 \quad (2.1.6)$$

Thus, the classical curvatures are

$$\kappa_x^c = -w_{,xx}^0 \quad \kappa_y^c = -w_{,yy}^0 \quad \kappa_{xy}^c = -2w_{,xy}^0 \quad (2.1.7)$$

Including transverse shear strains makes the curvatures

$$\kappa_x = -w_{,xx}^0 + \gamma_{xz,x}$$

$$\kappa_y = -w_{,yy}^0 + \gamma_{yz,y} \quad (2.1.8)$$

$$\kappa_{xy} = -2w_{,xy}^0 + \gamma_{xz,y} + \gamma_{yz,x}$$

2.2 STRAIN - DISPLACEMENT EQUATIONS

Following a Lagrangian description, the Green strain tensor, corresponding to finite deformations, is used to relate the strains to the displacements:

$$\begin{aligned}
 \epsilon_{11} &= u_{1,1} + \frac{1}{2} [(u_{1,1})^2 + (u_{2,1})^2 + (u_{3,1})^2] \\
 \epsilon_{22} &= u_{2,2} + \frac{1}{2} [(u_{1,2})^2 + (u_{2,2})^2 + (u_{3,2})^2] \\
 \epsilon_{33} &= u_{3,3} + \frac{1}{2} [(u_{1,3})^2 + (u_{2,3})^2 + (u_{3,3})^2] \\
 \epsilon_{23} &= u_{3,2} + u_{2,3} + u_{1,2}u_{1,3} + u_{2,2}u_{2,3} + u_{3,2}u_{3,3} \\
 \epsilon_{31} &= u_{3,1} + u_{1,3} + u_{1,1}u_{1,3} + u_{2,1}u_{2,3} + u_{3,1}u_{3,3} \\
 \epsilon_{12} &= u_{2,1} + u_{1,2} + u_{1,1}u_{1,2} + u_{2,1}u_{2,2} + u_{3,1}u_{3,2}
 \end{aligned} \tag{2.2.1}$$

According to the von Karman assumptions, in-plane displacements are assumed to be small and products of the in-plane displacement gradients are ignored. However, the transverse displacement gradient is not considered negligible. Using these assumptions, along with those developed in the preceding section, the strain-displacement relations become

$$\begin{aligned}
 \epsilon_x &= u_{,x} + \frac{1}{2} (w_{,x})^2 \\
 \epsilon_y &= v_{,y} + \frac{1}{2} (w_{,y})^2 \\
 \epsilon_z &= 0 \\
 \gamma_{xy} &= u_{,y} + v_{,x} + w_{,x}w_{,y} \\
 \gamma_{xz} &= u_{,z} + w_{,x} = \psi_x + w_{,x} \\
 \gamma_{yz} &= v_{,z} + w_{,y} = \psi_y + w_{,y}
 \end{aligned} \tag{2.2.2}$$

where eqn. (2.1.1) is used to evaluate $u_{,z}$ and $v_{,z}$. Eqn. (2.2.2) is sometimes called the von Karman strain tensor. Note that the transverse shear strains may be deduced from Fig. (2) or from the von Karman assumptions (eqn. 2.2.1). Using eqn. (2.2.1), the curvatures may be found in terms of the displacements:

$$\begin{aligned} \kappa_x &= u_{,xz} \\ \kappa_y &= v_{,yz} \\ \kappa_{xy} &= u_{,yz} + v_{,xz} \end{aligned} \tag{2.2.3}$$

2.3 STRESS - STRAIN RELATIONS

Following standard notation, the constitutive relations (giving stresses in terms of strains) may be written as

$$\sigma_i = C_{ij} \varepsilon_j \quad i, j = 1, 2, \dots, 6 \tag{2.3.1}$$

The stresses and strains given above are defined in terms of the standard tensor notation as:

$$\begin{aligned} \sigma_1 &\equiv \sigma_{11}, & \sigma_2 &\equiv \sigma_{22}, & \sigma_3 &\equiv \sigma_{33}, & \sigma_4 &\equiv \sigma_{23}, & \sigma_5 &\equiv \sigma_{31}, & \sigma_6 &\equiv \sigma_{12} \\ \varepsilon_1 &\equiv \varepsilon_{11}, & \varepsilon_2 &\equiv \varepsilon_{22}, & \varepsilon_3 &\equiv \varepsilon_{33} \\ \varepsilon_4 &\equiv \gamma_{23} \equiv 2\varepsilon_{23}, & \varepsilon_5 &\equiv \gamma_{31} \equiv 2\varepsilon_{31}, & \varepsilon_6 &\equiv \gamma_{12} \equiv 2\varepsilon_{12} \end{aligned} \tag{2.3.2}$$

Note that the engineering shear strain, γ_{ij} , is twice the tensor shear strain, ε_{ij} ($i \neq j$). This follows from the definition of tensor shear strain which simplifies the tensor form of the equations.

An important consideration is the form of the stress-strain curves. If stress is a linear function of strain, then the elements of

C_{ij} are all constants related to the slopes of the stress-strain plots. However, there are materials for which stress is not a linear (straight-line) function of strain. Such a relation is called a material nonlinearity and may be found, for example, in viscoelastic materials. Material nonlinearities are an interesting phenomenon which may be accounted for in a finite-element program such as the one used for this analysis. Due to time constraints, however, this work was restricted to linear elastic materials.

Furthermore, since the purpose of this work is to develop an accurate method for analyzing the transient response of laminated composite plates, only fiber-reinforced laminates are considered. This is justifiable by the fact that most laminates in use, especially in moving structures, fall into the category of fiber-reinforced laminates. As discussed in the first chapter, fiber-reinforced laminates are transversely isotropic within each layer. For transversely isotropic materials, the stress-strain relations reduce from eqn. (2.3.1) to

$$\begin{Bmatrix} \sigma_1 \\ \sigma_2 \\ \sigma_3 \\ \sigma_4 \\ \sigma_5 \\ \sigma_6 \end{Bmatrix} = \begin{bmatrix} C_{11} & C_{12} & C_{12} & 0 & 0 & 0 \\ & C_{22} & C_{23} & 0 & 0 & 0 \\ & & C_{22} & 0 & 0 & 0 \\ & & & \left(\frac{C_{22} - C_{23}}{2}\right) & 0 & 0 \\ & & & & C_{55} & 0 \\ & & & & & C_{55} \end{bmatrix} \begin{Bmatrix} \epsilon_1 \\ \epsilon_2 \\ \epsilon_3 \\ \gamma_{23} \\ \gamma_{31} \\ \gamma_{12} \end{Bmatrix} \quad (2.3.3)$$

where there are 5 independent constants.

2.4 EQUATIONS OF MOTION

The general nonlinear equations of motion for three-dimensional elasticity may be written

$$\begin{aligned}
 & \frac{\partial}{\partial x} \left[\sigma_1 \left(1 + \frac{\partial u}{\partial x} \right) + \sigma_6 \frac{\partial u}{\partial y} + \sigma_5 \frac{\partial u}{\partial z} \right] + \frac{\partial}{\partial y} \left[\sigma_6 \left(1 + \frac{\partial u}{\partial x} \right) + \sigma_2 \frac{\partial u}{\partial y} + \sigma_4 \frac{\partial u}{\partial z} \right] \\
 & + \frac{\partial}{\partial z} \left[\sigma_5 \left(1 + \frac{\partial u}{\partial x} \right) + \sigma_4 \frac{\partial u}{\partial y} + \sigma_3 \frac{\partial u}{\partial z} \right] + X_1 = \rho_0 \frac{\partial^2 u}{\partial t^2} \\
 & \frac{\partial}{\partial x} \left[\sigma_1 \frac{\partial v}{\partial x} + \sigma_6 \left(1 + \frac{\partial v}{\partial y} \right) + \sigma_5 \frac{\partial v}{\partial z} \right] + \frac{\partial}{\partial y} \left[\sigma_6 \frac{\partial v}{\partial x} + \sigma_2 \left(1 + \frac{\partial v}{\partial y} \right) + \sigma_4 \frac{\partial v}{\partial z} \right] \\
 & + \frac{\partial}{\partial z} \left[\sigma_5 \frac{\partial v}{\partial x} + \sigma_4 \left(1 + \frac{\partial v}{\partial y} \right) + \sigma_3 \frac{\partial v}{\partial z} \right] + X_2 = \rho_0 \frac{\partial^2 v}{\partial t^2} \quad (2.4.1) \\
 & \frac{\partial}{\partial x} \left[\sigma_1 \frac{\partial w}{\partial x} + \sigma_6 \frac{\partial w}{\partial y} + \sigma_5 \left(1 + \frac{\partial w}{\partial z} \right) \right] + \frac{\partial}{\partial y} \left[\sigma_6 \frac{\partial w}{\partial x} + \sigma_2 \frac{\partial w}{\partial y} + \sigma_4 \left(1 + \frac{\partial w}{\partial z} \right) \right] \\
 & + \frac{\partial}{\partial z} \left[\sigma_5 \frac{\partial w}{\partial x} + \sigma_4 \frac{\partial w}{\partial y} + \sigma_3 \left(1 + \frac{\partial w}{\partial z} \right) \right] + X_3 = \rho_0 \frac{\partial^2 w}{\partial t^2} + q(x, y, t)
 \end{aligned}$$

where X_i are the body forces, q is the transverse loading, and ρ_0 is the density. As in the so-called von Karman assumptions, the in-plane displacements are assumed to be small. Consequently, the spatial derivatives of u and v are neglected. Taking into account eqn. (2.1.1), and remembering that shear stresses and strains are assumed constant through the thickness, the equations of motion become

$$\begin{aligned}
 \sigma_{1,x} + \sigma_{6,y} &= \rho_0 [u^0_{,tt} + z\psi_{x,tt}] \\
 \sigma_{6,x} + \sigma_{6,y} &= \rho_0 [v^0_{,tt} + z\psi_{y,tt}] \quad (2.4.2) \\
 [\sigma_{1w,x} + \sigma_{6w,y}]_{,x} + [\sigma_{6w,x} + \sigma_{2w,y}]_{,y} + \sigma_{5,x} + \sigma_{4,y} &= \rho_0 w_{,tt} \\
 &+ q(x, y, t)
 \end{aligned}$$

where body forces have been neglected. Two moment equations of motion are obtained by multiplying the first two equations by z , the transverse coordinate measured from the reference surface. When these 5 equations are integrated through the thickness, the equations of motion in terms of stress and moment resultants are obtained:

$$\begin{aligned}
 N_{1,x} + N_{6,y} &= P u_{,tt}^0 + R \psi_{x,tt} \\
 N_{6,x} + N_{2,y} &= P v_{,tt}^0 + R \psi_{y,tt} \\
 [N_{1w,x} + N_{6w,y}]_{,x} + [N_{6w,x} + N_{2w,y}]_{,y} + Q_{5,x} + Q_{4,y} &= P w_{,tt} \\
 &+ q(x,y,t)
 \end{aligned} \tag{2.4.3}$$

$$\begin{aligned}
 M_{1,x} + M_{6,y} - Q_5 &= R u_{,tt}^0 + I \psi_{x,tt} \\
 M_{6,x} + M_{2,y} - Q_4 &= R v_{,tt}^0 + I \psi_{y,tt}
 \end{aligned}$$

P, R, I are called the normal, coupled normal-rotatory, and rotatory inertia, respectively, and are given by

$$(P, R, I) = \int_0^h (1, z, z^2) \rho_0 dz \tag{2.4.4}$$

Following standard plate notation, the stress and moment resultants are defined as

$$\begin{aligned}
 (N_1, N_2, N_6) &= \int_0^h (\sigma_1, \sigma_2, \sigma_6) dz \\
 (Q_5, Q_4) &= \int_0^h (\sigma_5, \sigma_4) dz \\
 (M_1, M_2, M_6) &= \int_0^h (\sigma_1, \sigma_2, \sigma_6) z dz
 \end{aligned} \tag{2.4.5}$$

where the thickness of the plate is h . These resultants are shown in Fig. (3).

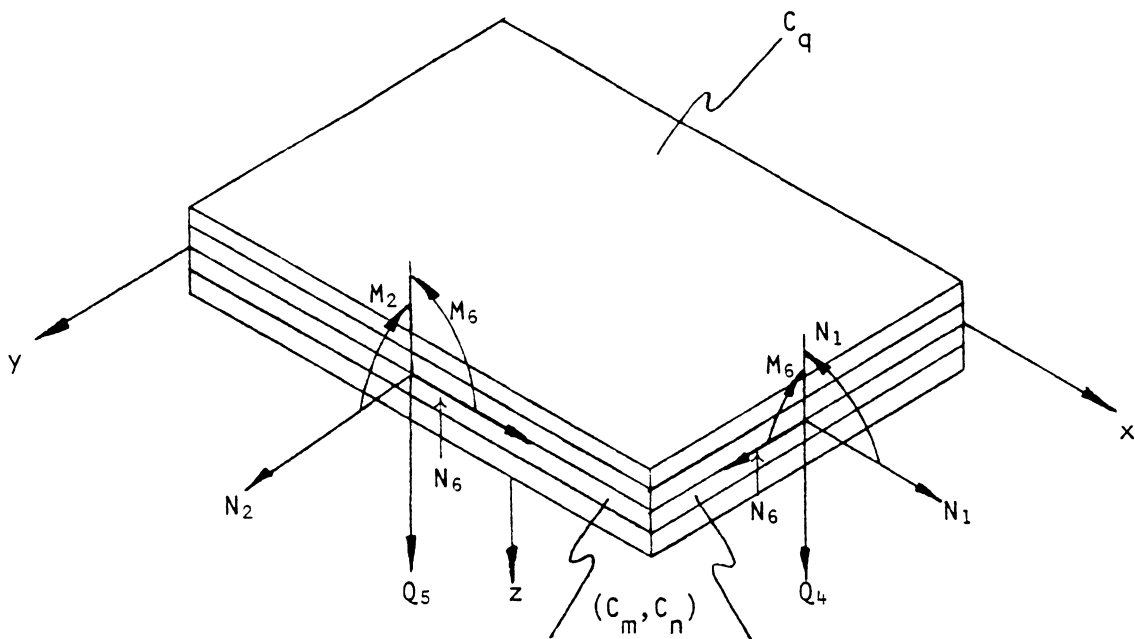


Figure 3 Stress Resultants and Surfaces of Integration.

Stresses and moments are positive as shown. C_q is the surface for the applied load and C_m, C_n is the surface for the stress and moment resultants.

Chapter III

DEVELOPMENT OF THE COMPUTER PROGRAM

3.1 COMMENTS

It is far beyond the scope of this paper to present in detail the procedure used to solve the governing equations developed in Chapter II. The purpose of this chapter is to provide a brief outline of the development and implementation of the computer program used to obtain approximate solutions to the equations of motion. A flow chart of the program is provided in Appendix B, and a listing of the code is in Appendix C. Results of analyses undertaken with this program are presented later.

3.2 VARIATIONAL FORMULATION

The first step in developing the program is to write the equations of motion in variational form, using as the 'variational principle' the principle of minimum potential (strain) energy. The strain energy may be thought of as the product of the stress and the displacement. Consequently, the equations of motion, eqns. (2.4.3), multiplied by the appropriate displacements, are integrated over the domain (the reference surface) to obtain the strain energy, and then the variation of the strain energy is set equal to zero:

$$\begin{aligned}
\delta(\pi) = 0 = \int_{\Omega} \left\{ \delta u^0 [N_{1,x} + N_{6,y} - Pu^0_{,tt} - R\psi_{x,tt}] \right. \\
+ \delta v^0 [N_{6,x} + N_{2,y} - Pv^0_{,tt} - R\psi_{y,tt}] + \delta w^0 [(N_{1w,x} + N_{6w,y})_{,x} \\
+ (N_{6w,x} + N_{2w,y})_{,y} + Q_{5,x} + Q_{4,y} - Pw_{,tt} - q] \\
+ \delta\psi_x [M_{1,x} + M_{6,y} - Q_5 - Ru^0_{,tt} - I\psi_{x,tt}] \\
\left. + \delta\psi_y [M_{6,x} + M_{2,y} - Q_4 - Rv^0_{,tt} - I\psi_{y,tt}] \right\} dx dy \quad (3.1.1)
\end{aligned}$$

where π is the strain energy.

The terms containing N_i , M_i , and Q_i are now replaced using the product rule. For example,

$$\delta u^0 N_{1,x} = [\delta u^0 N_1]_{,x} - N_1 \delta u^0_{,x} \quad (3.1.2)$$

Similarly, the other N , M , and Q terms may be replaced using the product rule. Eqn. (3.2.1) may be written

$$\begin{aligned}
0 = \int_{\Omega} \left\{ \delta u^0 [Pu^0_{,tt} + R\psi_{x,tt}] + \delta u^0_{,x} N_1 + \delta u^0_{,y} N_6 + \delta v^0 [Pv^0_{,tt} + R\psi_{y,tt}] \right. \\
+ \delta v^0_{,x} N_6 + \delta v^0_{,y} N_2 + \delta w Pw_{,tt} + \delta w_{,x} Q_5 + \delta w_{,y} Q_4 \\
+ \delta w_{,x} (N_{1w,x} + N_{6w,y}) + \delta w_{,y} (N_{6w,x} + N_{2w,y}) \\
+ \delta\psi_x [Ru^0_{,tt} + I\psi_{x,tt} + Q_5] + \delta\psi_{x,x} M_1 + \delta\psi_{x,y} M_6 \\
+ \delta\psi_y [Rv^0_{,tt} + I\psi_{y,tt} + Q_4] + \delta\psi_{y,x} M_6 + \delta\psi_{y,y} M_2 \left. \right\} dx dy \\
- \int_{\Omega} \left\{ [\delta u^0 N_1]_{,x} + [\delta u^0 N_6]_{,y} + [\delta v^0 N_6]_{,x} + [\delta v^0 N_2]_{,y} \right. \\
+ [\delta w (N_{1w,x} + N_{6w,y})]_{,x} + [\delta w (N_{6w,x} + N_{2w,y})]_{,y} \\
+ [\delta w Q_5]_{,x} + [\delta w Q_4]_{,y} + q\delta w + [\delta\psi_x M_1]_{,x} + [\delta\psi_x M_6]_{,y} + \delta\psi_x Q_5 \\
\left. + [\delta\psi_y M_6]_{,x} + [\delta\psi_y M_2]_{,y} + \delta\psi_x Q_4 \right\} dx dy \quad (3.1.3)
\end{aligned}$$

Using the divergence theorem, some of the volume integrals in eqn.

(3.2.3) may be converted to surface integrals. Specifically,

$$\begin{aligned}
 & \int_{\Omega} \left\{ [\delta u^0 N_1]_{,x} + [\delta u^0 N_5]_{,y} + [\delta v^0 N_6]_{,x} + [\delta v^0 N_2]_{,y} \right. \\
 & \quad \left. + q \delta w + [\delta \psi_x M_1]_{,x} + [\delta \psi_x M_6]_{,y} + [\delta \psi_y M_6]_{,x} + [\delta \psi_y M_2]_{,y} \right\} dx dy \\
 & = \int_{C_n} \delta (u_n N_n + \delta u_s N_{ns}) ds + \int_{C_q} \delta w q ds \\
 & \quad + \int_{C_m} (\delta \psi_n M_n + \sigma \psi_s M_{ns}) ds \tag{3.1.4}
 \end{aligned}$$

where C_n , C_q , and C_m are shown in Fig. 3.

The right hand side of eqn. (3.1.4) clearly indicates the boundary conditions. On each face of the four-sided (quadrilateral) element, specify exactly one of each of the following pairs:

$$u_n \quad \text{or} \quad N_n$$

$$u_{ns} \quad \text{or} \quad N_{ns}$$

$$w \quad \text{or} \quad q$$

(3.1.5)

$$\psi_n \quad \text{or} \quad M_n$$

$$\psi_{ns} \quad \text{or} \quad M_{ns}$$

where the subscript 'n' indicates normal and 's' indicates tangential.

3.3 THE FINITE ELEMENT PROGRAM

Time and space constraints prevent describing the finite-element method (FEM) in any more detail than a rudimentary discussion. In order to provide the most useful information in the limited space available, the structure and execution of the computer program used in the analysis is outlined in appendices A, B, and C. The rest of this chapter outlines the procedures used in the program and discusses certain areas where engineering judgement is required.

3.3.1 BRIEF OUTLINE OF THE FEM

As used in this analysis, the FEM consists of the following general steps

1. Write the governing equations for the medium and then state the minimum potential (strain) energy using standard variational procedures.
2. Discretize the domain into 'finite elements'.
3. Select approximation functions (often called the 'shape functions') to be used to approximate the solution in each element.
4. Derive the element governing equations using the equations from step 1 along with the approximation functions from step 3.
5. Assemble the element governing equations from step 4 into global governing equations. A set of simultaneous equations is obtained which may be written in the form

$$[M]\{\ddot{\Delta}\} + [K]\{\Delta\} = F(t) \quad (3.3.1)$$

where $[M]$ is the 'mass matrix', $[K]$ is the 'stiffness matrix', $\{\Delta\}$ is the vector of node-point displacements, $\{\ddot{\Delta}\}$ is the vector of node-point accelerations, and $F(t)$ is the node-point force vector. This is a 'displacement formulation'.

6. Reformulate the equations using the time-marching scheme outlined in the next section. This produces a set of simultaneous equations which may be written

$$[K']\{\Delta\} = F'(t) \quad (3.3.2)$$

7. Apply the boundary conditions to eqn. (3.3.2).
8. Solve for the unknown displacements in eqn. (3.3.2).
9. Solve for the so-called secondary quantities; e.g., use the strain-displacement relations to find the strains, then use the stress-strain relations to find the stresses.

3.4 THE TIME-MARCHING SCHEME

Eqns. (3.3.1) are valid at any particular time t . In order to integrate eqns. (3.3.1), Newmark's direct integration technique is employed. Using this technique, the displacements and accelerations are found at the discrete times $t_0 = 0$, $t_1 = \delta t$, $t_2 = 2\delta t, \dots, t_n = n\delta t$. The velocities $\{\dot{\Delta}\}$ and displacements $\{\Delta\}$ are found at time step $k+1$ (i.e., $t = (k+1)\delta t$) by the following assumed expressions

$$\{\dot{\Delta}\}_{k+1} = \{\dot{\Delta}\}_k + [(1 - \alpha)\{\ddot{\Delta}\}_k + \alpha\{\ddot{\Delta}\}_{k+1}]\delta t \quad (3.4.1)$$

$$\{\Delta\}_{k+1} = \{\Delta\}_k + \{\dot{\Delta}\}_k\delta t + \left[\left(\frac{1}{2} - \beta\right)\{\ddot{\Delta}\}_k + \beta\{\ddot{\Delta}\}_{k+1}\right](\delta t)^2$$

where the subscripts refer to the quantity at that time step and α and β are constants used to obtain accuracy and stability. α is determined from β by the expression

$$\beta = \frac{1}{4} \left(\frac{1}{2} + \alpha \right)^2 \quad (3.4.2)$$

For linear analysis, the choice $\alpha = \frac{1}{2}$ and $\beta = \frac{1}{4}$ has been shown to be unconditionally stable. No similar results for nonlinear analysis have been reported in the literature.

A brief investigation of the effect of varying α and β in the present nonlinear analysis was carried out by running the same problem with several different values for the two parameters. The results are shown in Fig. (4).

In Fig. (4), the effect of α and β on stability is shown. It is clear that for $\alpha = 0.1, 0.2,$ and $0.3,$ the solution becomes unstable before the peak deflection is reached. For $\alpha = 0.4,$ the solution becomes unstable near the end of the first deflection cycle. For $\alpha = 0.5,$ the solution maintains stability throughout the deflection cycle. In all of the results reported later, a value of $\alpha = 0.5$ was used and assumed to be both stable and accurate.

The size of the time-step used in the time-marching equations is also important for stability and accuracy. Too small a time-step will add to the cost, perhaps significantly, but too large a time-step may give unstable or inaccurate answers. At any given discrete time during

EFFECT OF ALPHA - ALPHA = .1, .2, .3, .4, .5 (NEWMARK)
 TWO-LAYER CROSS-PLY, UDL, SS, SQ. PLATE WITH $A/H=10$
 $QBAR=50$, $E1/E2=25$

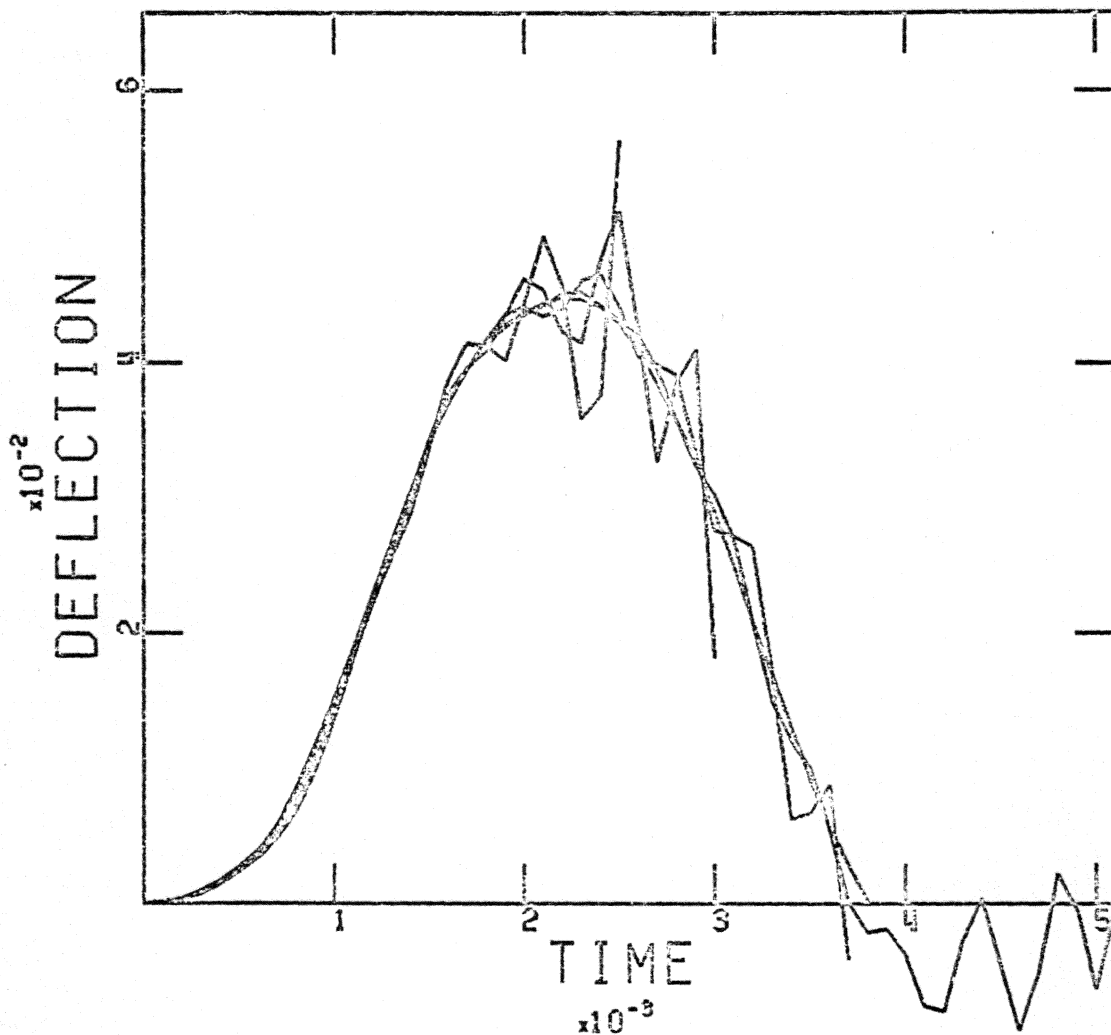


Figure 4 Effect of α on the Stability of the Solution.

The data for these cases is given in eqn. (4.4.1), except for the variation of α . Note that as α increases, the solution maintains stability longer through the cycle. For $\alpha = 0.5$, the solution is stable throughout the cycle.

the time-marching algorithm, the program must iterate to find the nonlinear solution. Thus, the total number of iterations required to integrate the equations of motion for a specific problem is the sum of the nonlinear iterations required for each discrete time during the time march. If the time-step is too small, the number of total iterations may be high even though the number of iterations at each discrete time may be low. Increasing the size of the time-step may reduce the total number of iterations by reducing the number of discrete times at which a solution is sought. However, if the time-step is too large, the program may require enough extra iterations to converge at each discrete time that the total number of iterations will be higher than the total for a smaller time-step. Therefore, the size of the time-step may have a profound effect on the efficiency (measured by the total number of iterations) of the program.

Time-steps used in this analysis were determined in the following manner. The solution was found using an initial time-increment value of $(\delta t)_0$. The solution was then calculated using a smaller value for δt_0 and the solutions from the two different time-increment values were compared. If necessary, smaller and smaller time-increments were used until the solutions converged. When the solutions were essentially identical for two different time-increment values, stability and accuracy were assumed. Every result reported herein was obtained in this fashion and is assumed to represent a stable and accurate solution. Comparisons with well-known solutions for certain special cases are reported in Chapter 4 and indicate that this method is indeed accurate.

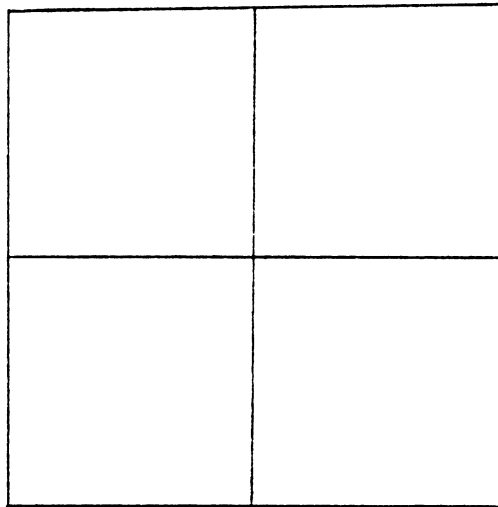
3.5 SPECIAL CONSIDERATIONS

The following observations concerning the actual programming are presented without pretense to a complete explanation.

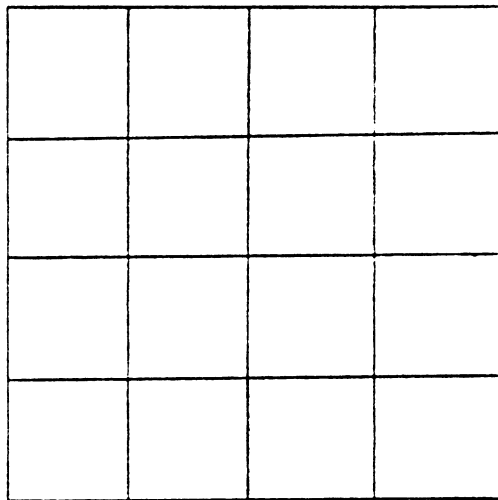
Discretization is often the most subjective phase of any finite-element analysis. In this analysis, each node was allowed five degrees-of-freedom (D.O.F.); u, v, w, ψ_x, ψ_y . Considering eqn. (3.3.1), the finite-element method eventually reduces to the solution of a system of simultaneous equations, of the order of the total number of D.O.F. Since every node adds five to the order of the system, there is an obvious savings (which may be astronomical!) to be gained by using as few nodes as possible. On the other hand, having too few nodes may adversely affect accuracy. In fact, since the program iterates to find a solution within a user-supplied error bound, too few nodes may lead to a large enough increase in the number of iterations to offset or even exceed the savings of a small-order system. For the purpose of this analysis, the element break-up shown in Figure (5a) was used. A finer mesh is shown in Figure (5b). The mesh in Figure (5b) cost approximately 10 times as much to execute as the mesh in Figure (5a), yet the results were indistinguishable.

The elements of the mass [M] and stiffness [K] matrices are given in Appendix A. The derivation involves rather lengthy manipulations and is not included.

The five boundary conditions for any particular node are given in eqn. (3.1.5). In Figure (6a), the boundary conditions are shown for



(a)



(b)

Figure 5 Finite Element Mesh.

For the test cases used, the mesh in (a) produced results identical to the mesh in (b) but at approximately 1/10 the cost.

the mesh used in this analysis. An alternate formulation of boundary conditions is also possible and is shown in Figure (6b). The alternate form produces a significant difference in both the magnitude and timing of the response, as shown in Figure (7). The boundary conditions in Figure (6a) are generally accepted as correct, and a comparison of results obtained using these boundary conditions with results obtained from an exact solution for a linear homogeneous plate shows excellent agreement (see Figure 8).

A flow chart of the program is included in Appendix B, and a listing of the program is provided in Appendix C.

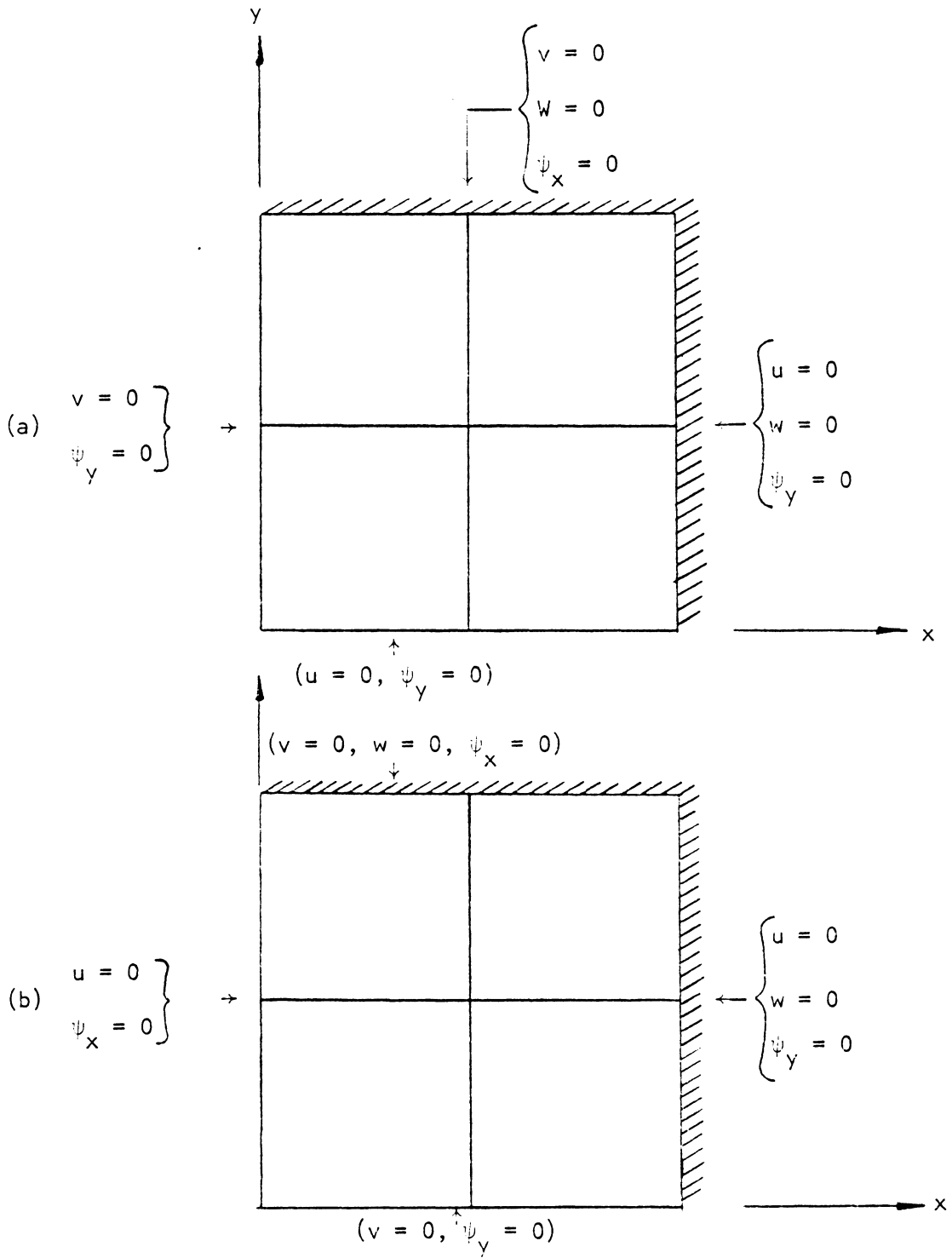


Figure 6 Alternate Forms of the Boundary Conditions.

Results are given in Figure (7).

EFFECT OF BOUNDARY CONDITIONS - TWO FORMS IN FIG. 6
TWO-LAYER CROSS-PLY, UDL, SS, SQ. PLATE WITH $A/H=10$
 $QBAR=50$, $E1/E2=25$

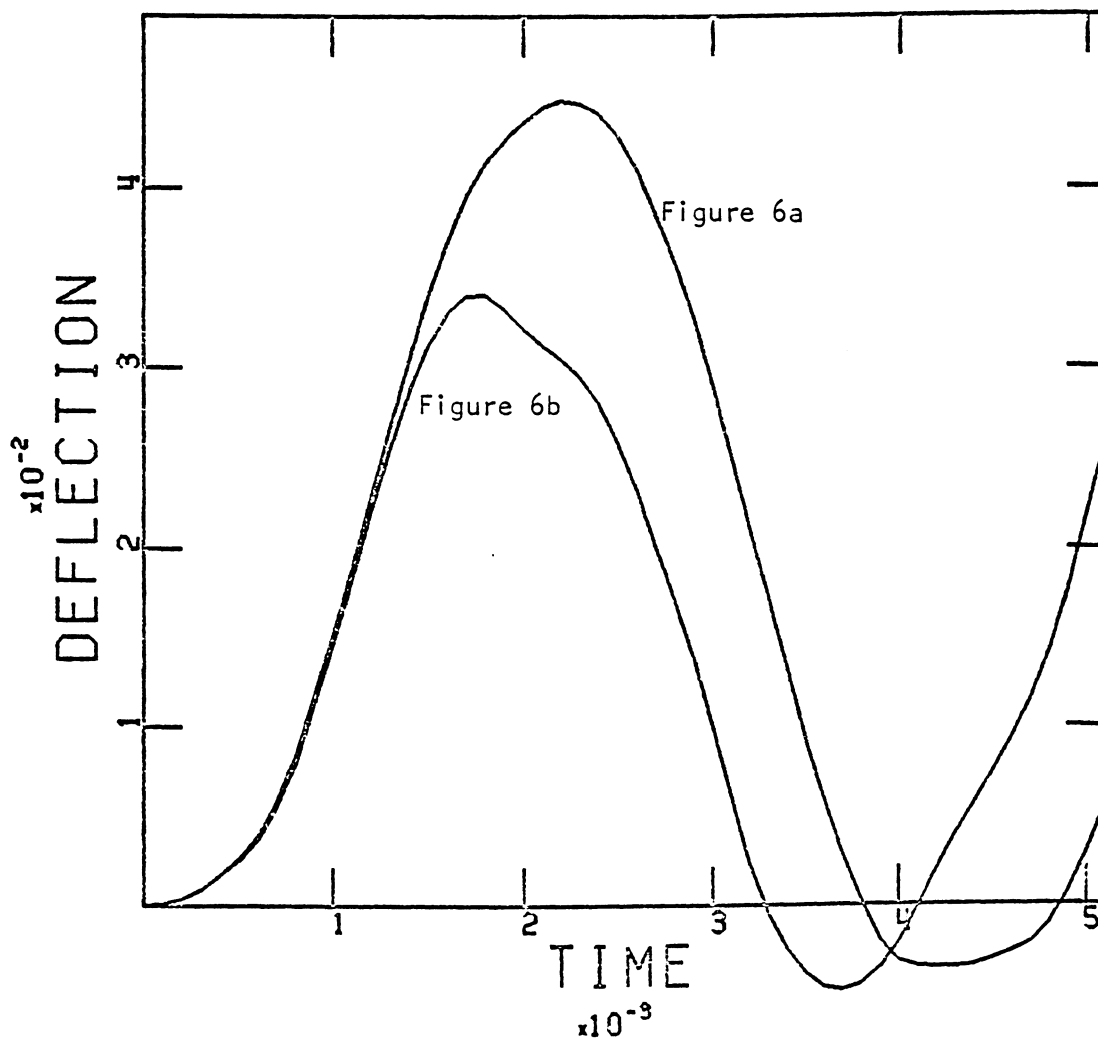


Figure 7 Comparison of Results Using Different Boundary Conditions. Note that (a) and (b) from Figure 6 give markedly different results. The conditions in Figure (6a) are generally regarded as correct.

Chapter IV

VERIFICATION AND RESULTS

4.1 COMMENTS

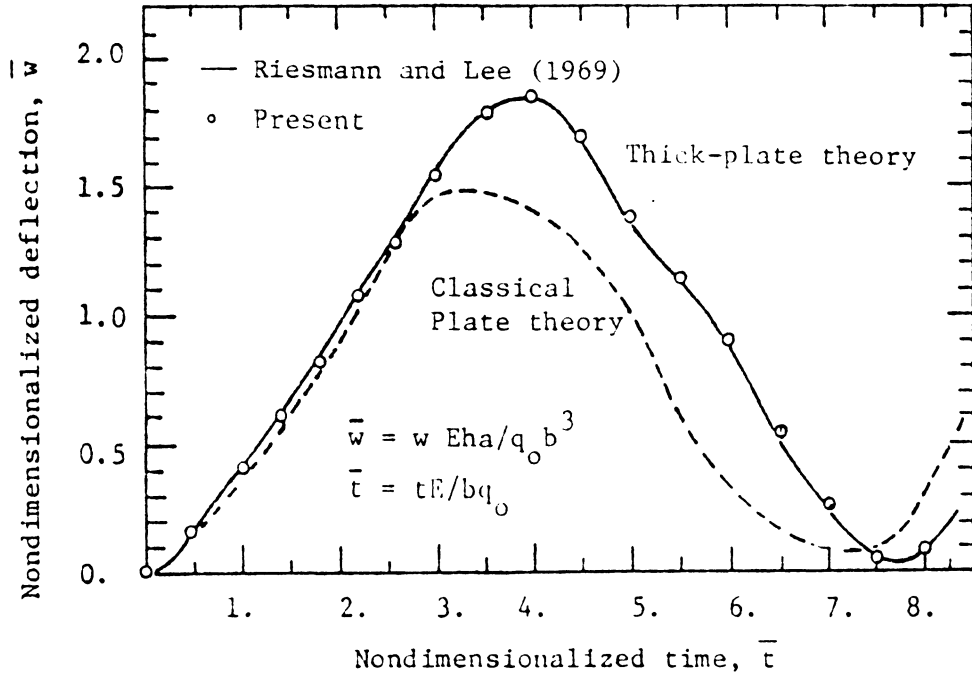
In this chapter, the accuracy of the program is established and then certain parametric effects are investigated. The accuracy will be demonstrated by comparing results obtained using this program with those available in the literature. Excellent agreement is evident. Next, the effect of the transverse shear constant and the rotatory inertia is illustrated for specific data cases (the effect is different for every data case). Finally, the effects of load magnitude, material orthotropy, plate aspect ratio, plate thickness, and lamination scheme are reported.

4.2 VERIFICATION

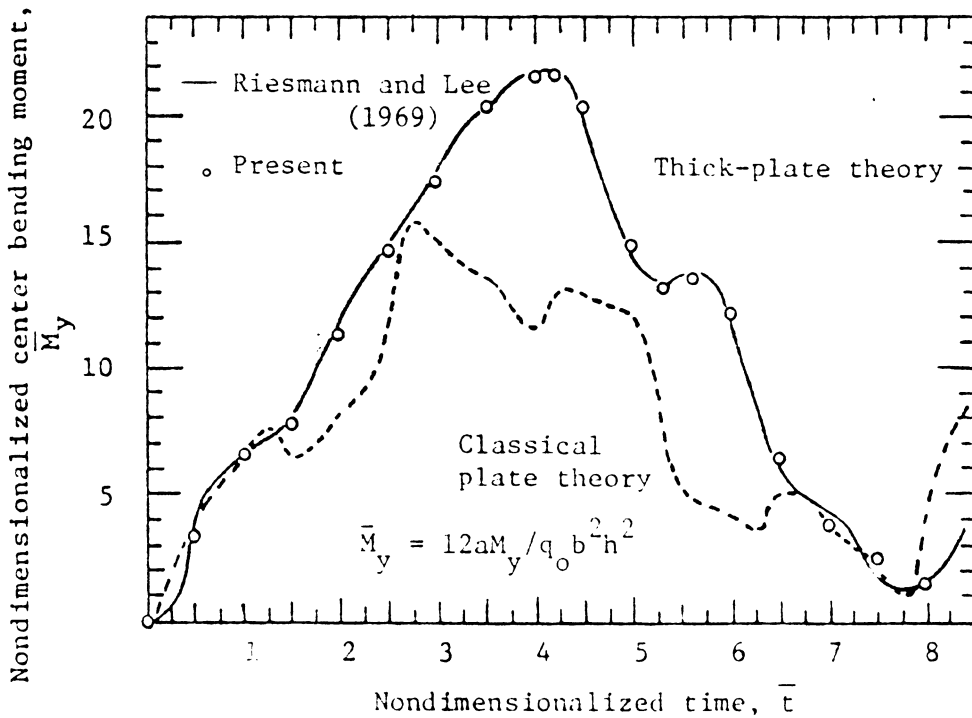
The program accuracy was initially checked against linear isotropic solutions. In Figure (9), the results from this program are plotted along with a classical thin-plate theory solution due to Volterra and Zachmanoglou (11) and an analytical thick-plate solution due to Reismann and Lee (12).

The data for this program was as follows:

$$\begin{aligned} a = 4, \quad b = 2, \quad h = 0.2, \quad \rho = 1, \quad \delta t = 0.1, \quad \nu = 0.3, \\ E = 1, \quad q_0 = 10 \end{aligned} \tag{4.2.1}$$



(a) Deflection versus time



(b) Bending moment versus time

Figure 2 The transient response of a simply supported rectangular isotropic plate subjected to suddenly applied patch loading at the center (DATA 2, 4x4 mesh, $\Delta t = 1$)

Here a and b are the length and width; h is the thickness; ρ , ν , E are the density, Poisson's ratio, and Young's modulus; q_0 is the uniform applied load magnitude; and δt is the time-step size. Note that the ratio of b/h is only 10, whereas classical plate theory generally assumes a ratio of at least 10. Two important results are evident in Figure (9). First, the classical theory is inadequate for predicting thick-plate response. Second, the present program shows excellent agreement with the analytical thick-plate solution.

Akay (13) obtained both linear and nonlinear results for isotropic plates using a mixed formulation. In Figure (10), linear results from this program are compared with Akay's linear results for a simply supported square plate subjected to uniform pulse loading. The data for this case was

$$a = b = 25 \text{ cm}, \quad h = 5 \text{ cm}, \quad \delta t = 5, 10 \mu \text{ sec}, \quad q_0 = \frac{N}{\text{cm}^2},$$

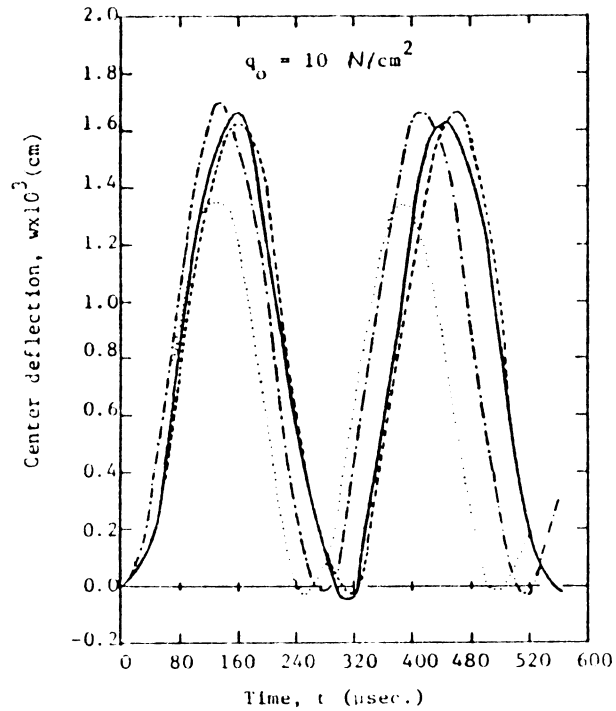
$$\rho = 8 \times 10^{-6} \frac{\text{Ns}^2}{\text{cm}^2}, \quad \nu = 0.25, \quad E = 2.1 \times 10 \frac{6N}{\text{cm}^2} \quad (4.2.2)$$

Although the peak values show good agreement, note that there is a small phase difference between the two solutions. Overall, agreement is good. Again, the classical plate theory is presented to illustrate the significant error which may occur if transverse shear strains are neglected.

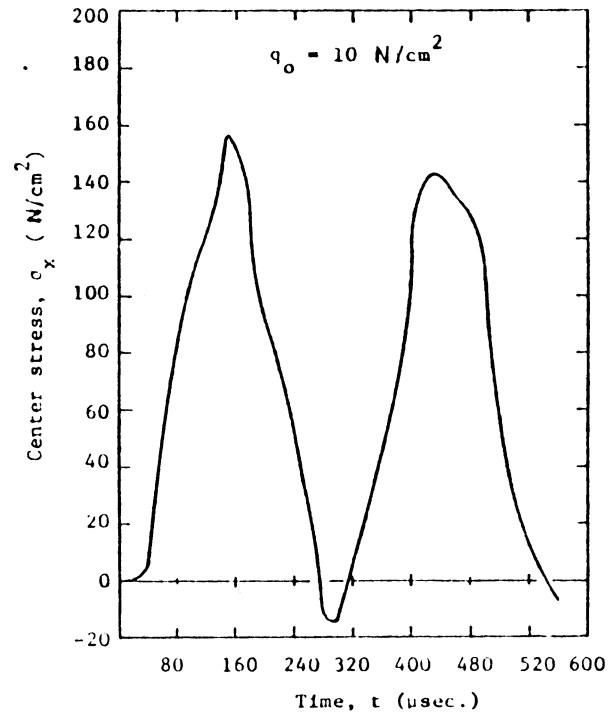
As a final verification, a nonlinear analysis was performed and the results were compared to those reported by Akay for a simply supported square plate subjected to uniform pulse loading. The data for this problem was as follows:

$$a = b = 243.8 \text{ cm}, \quad h = 0.635 \text{ cm}, \quad \nu = 0.25, \quad E = 7.031 \times 10^5 \frac{N}{\text{cm}^2},$$

$$\rho = 2.547 \times 10^{-6} \frac{\text{Ns}}{\text{cm}^2}, \quad q_0 = 4.882 \times 10^{-4} \frac{N}{\text{cm}^2}, \quad \delta t \leq 0.005 \text{ s} \quad (4.2.3)$$



(a) Center deflection



(b) Center stress

Figure 1. Transient response of a simply supported square plate subjected to uniform pulse loading (DATA 1, 2×2 mesh, $\Delta t = 5 \mu$ sec.)

LEGEND: present FEM $\Delta t = 10 \mu$; mixed FEM (Akay (1980)) $\Delta t = 5 \mu$
 $\Delta t = 5 \mu$

The results are plotted in Figure (11a), along with classical results due to Volterra and Zachmanoglou. Excellent agreement between the two nonlinear results are evident, although the present program predicts a slightly higher peak deflection than Akay. Note that the classical theory predicts a much larger response and a longer period. This difference may be attributed to the midplane stretching. The nonlinear results include the effect of midplane stretching, which increases the plate's bending stiffness because force is required to stretch the midplane while the plate is bending. The classical theory ignores this effect, making the plate appear less stiff. The 'stiffer' plate from the nonlinear analysis has a higher frequency and a lower peak deflection, as expected.

In Figure (11b), the results for several load magnitudes are compared with Akay. Excellent agreement was obtained. Note that the peak deflections form a nonlinear curve, clearly exhibiting the effect of midplane stretching. As the deflection increases, the plate becomes stiffer in bending because of the extra force required to stretch the midplane. Using classical linear theory, the peak deflection is a linear function of the load magnitude.

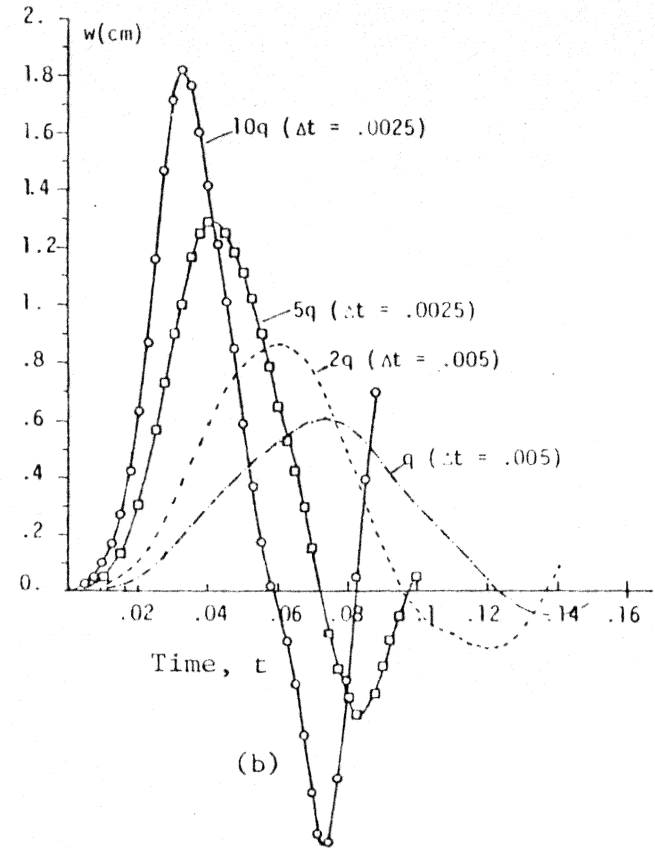
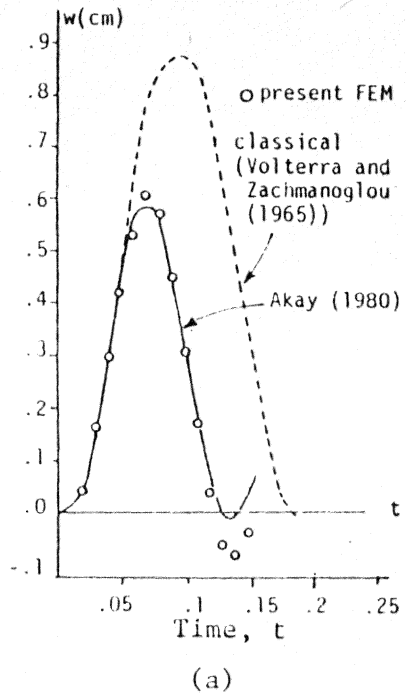


Figure 10 Comparison with Nonlinear Results from AKay.

Nonlinear transient response of a simply supported square plate under a uniformly distributed load.

Data is from eqn. 4.2.3.

4.3 EFFECT OF ROTATORY INERTIA AND TRANSVERSE SHEAR CONSTANT

In this section, the effect of different transverse shear constants and the effect of including rotatory inertia are illustrated. It is important to recall from the previous discussion that these effects are highly dependent on the particular problem for which they are investigated. Specifically, in the case of transverse shear constant the effects are more pronounced when the transverse shear constant is small compared to the in-plane Young's moduli. Rotatory inertia effects are more pronounced in thick plates or in large deflection analysis. Either effect may or may not be significant in any particular problem. It is this uncertainty which makes including these effects so important in analysis work.

In Figure (11), the effects of the transverse shear constant are illustrated for a specific material and a specific load. The material properties for this case correspond to a Graphite-Epoxy plate with a 64% fiber volume fraction. The data for this comparison is as follows:

$$E_1 = 22.2 \text{ msi}, \quad E_2 = 1.54 \text{ msi}, \quad a = b = 1 \text{ in}, \quad h = 0.1 \text{ in}$$

$$\text{Two-layer, cross-ply} \quad \bar{q} = \frac{q_0 a^4}{E_2 h^4} = 15 \quad (4.3.1)$$

$$\text{CASE 1: } G_{23} = G_{12} = G_{13} = 0.98 \text{ msi}$$

$$\text{CASE 3: } G_{12} = G_{13} = 0.98 \text{ msi}, \quad G_{23} = 0.54 \text{ msi}$$

Note that the difference between the two predicted responses in Figure (11) is obvious, but not too large. Again, it should be reiterated that

EFFECT OF TRANSVERSE SHEAR CONSTANT - TWO CASES
 CASE (1): $G_{23} = G_{12}$, CASE (2): $G_{23} = \frac{1}{2} G_{12}$
 TWO-LAYER CROSS-PLY, UDL, SS, SQ. PLATE WITH $A/H=10$

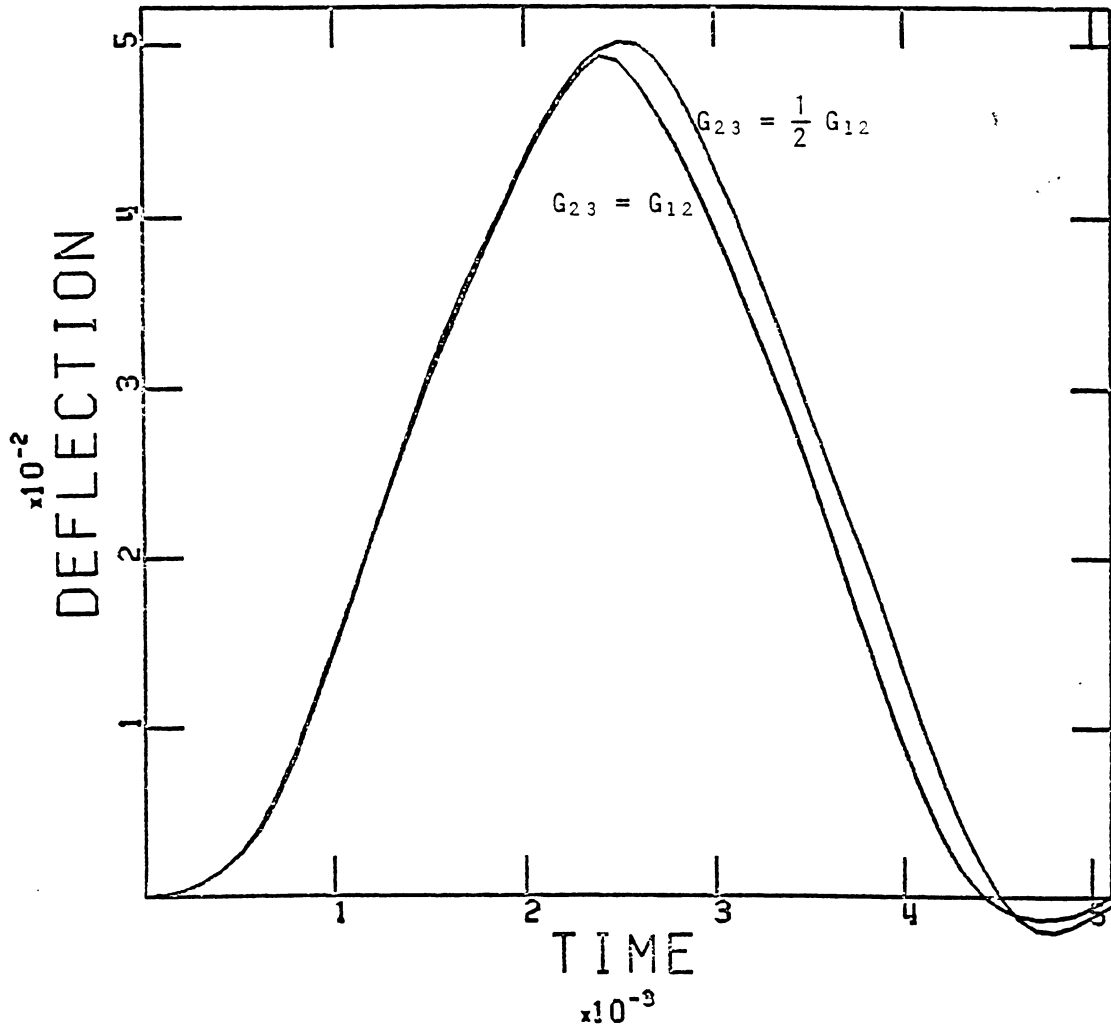


Figure 11 Effect of Transverse Shear Constant--A Specific Example.
 Data for these cases is presented in eqn. (4.3.1), and corresponds to Graphite-Epoxy with a 64% fiber volume fraction. Note that the effect may be greater or less for other data cases.

the difference may be greater or smaller for another data case, and it is precisely this uncertainty which necessitates including the transverse shear deformation in the analysis.

The effect of suppressing the rotatory inertia term (i.e., artificially forcing I to zero in the equations of motion) is illustrated in Figure (12). The data for this case is given below:

$$\begin{aligned} E_1 &= 25 \times 10^6, & E_2 &= 1 \times 10^6, & \rho &= 1, & \nu &= 0.25 \\ G_{12} &= G_{13} = G_{21} = G_{23} &= 0.5 \times 10^6, & a &= b = 1, & h &= 0.1 \\ \text{Two-layer, cross-ply, } \bar{q} &= \frac{q_0 a^4}{E_2 a^4} = 100 \end{aligned} \tag{4.3.2}$$

Simply supported, uniformly distributed load

For this data case, the effect of rotatory inertia is quite pronounced. With the rotatory inertia suppressed, the maximum predicted deflection is much smaller because the effect of the inertia of rotation is ignored. Only the transverse inertia is accounted for. In small deflection analysis, the rotations are small enough that often the rotatory inertia may be ignored without significantly affecting the predicted response. However, if the deflections are large, the inertia of the rotations may have a greater effect on the solution, as illustrated in Figure (12). The exact contribution of the rotatory inertia will be different for various problems. Again, it is this uncertainty which requires rotatory inertia to be included in the analysis.

The effect of including the geometric nonlinearities is amply illustrated in the previous section and is not repeated here.

EFFECT OF ROTARY INERTIA - I SET TO ZERO IN ONE CASE
 TWO-LAYER CROSS PLY, UDL, SS, SQ. PLATE WITH $A/H=10$
 $QBAR=100$, $E1/E2=25$

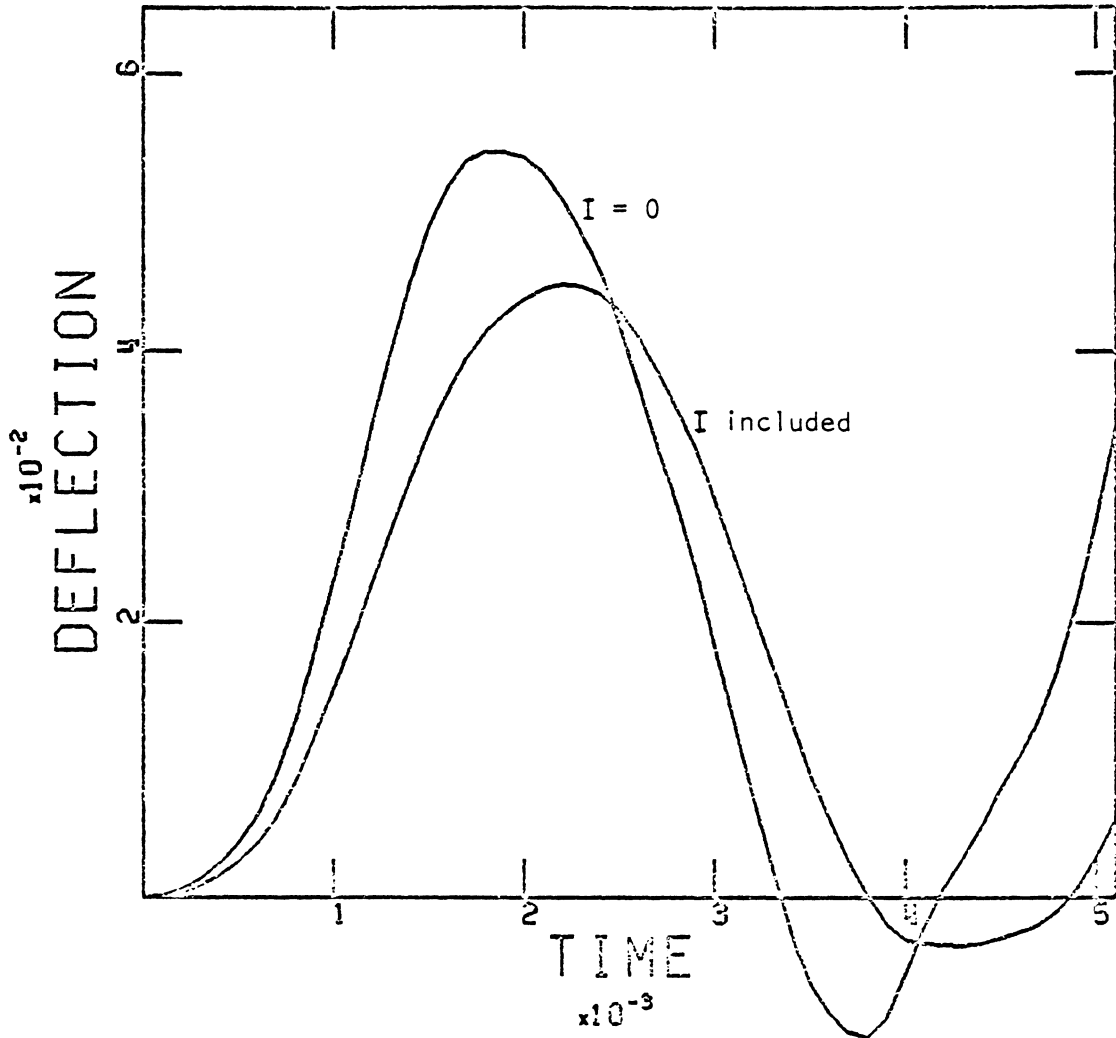


Figure 12 Effect of Rotary Inertia in a Specific Example.

The data for these cases is given in eqn. (4.3.2).

There is an interesting interaction between the effects of the transverse shear constant and the rotatory inertia. The rotatory inertia is much more pronounced in large deflection analysis and tends to mask the effect of transverse shear deformation in large-deflection problems. On the other hand, the rotatory inertia may be negligible for small-deflection analysis whereas the transverse shear deformation effect becomes much more pronounced. Thus, the effect of one of these considerations may be hidden by the effect of the other in any given problem. Note that in Figure (11), the normalized load magnitude \bar{q} is 15, but in Figure (12) the \bar{q} is 100. A run using the data for Figure (11) with the rotatory inertia suppressed produced a negligible difference from the curve in Figure (11); a run with the different transverse shear constants using q of 100 gave identical results for the two constants. It is essential to include both effects since the outcome for a specific case cannot be predicted in advance.

4.4 PARAMETRIC RESULTS

With the program's accuracy verified in the previous section, a study of the effects of various parameters is presented in this section. The mesh shown in Figure (5a) was used in all of these cases, along with the following 'base' data:

$$\bar{q} = \frac{q_0 a^4}{E_2 h^4} = 50, \quad \rho = 1, \quad E_2 = 1 \times 10^6$$

$$E_1 = 25 \times 10^6, \quad G_{12} = G_{13} = G_{23} = 0.5 \times 10^6, \quad a = b = 1, \quad h = 0.1$$

(4.4.1)

Two-layer, cross-ply, simply supported, uniformly distributed load

In Figure (13), the effect of the load magnitude is demonstrated. As discussed in the previous section, the plate becomes stiffer in bending as the deflection increases. This effect is not present in a linear analysis, and indicates the need to include geometric nonlinearities in large-deflection or thick-plate analyses.

The effect of material orthotropy is plotted in Figure (14). As expected, the plate becomes stiffer for higher ratios of E_1/E_2 since E_1 is increased while other parameters are held constant. The effect of including transverse shear strains is to produce a larger deflection than the linear theory, especially at higher ratios of E_1/E_2 . As discussed in Chapter I, the effect of transverse shear strains increases as the in-plane Young's moduli increase relative to the transverse shear stiffness.

In Figure (15), the effect of plate aspect ratio is plotted. Increasing the length of the plate reduces its stiffness under constant load, and this is indicated in Figure (15). As the plate aspect ratio increases, the period increases and the peak deflection increases.

Figure (16) shows the effect of lamination scheme on the response. Note that the peak deflection is considerably higher for a two-layer cross-ply plate than for any two-layer angle-ply plate. In addition, the period is longer for the cross-ply plate. Clearly, the cross-ply plate is not as stiff as the angle-ply plate.

EFFECT OF LOAD MAGNITUDE - $\bar{Q} = 15, 50, 75$
 TWO-LAYER, CROSS-PLY, UDL, SS, SO. PLATE WITH $A/H=10$
 $\text{ALPHA}=0.5, E_1/E_2=25$

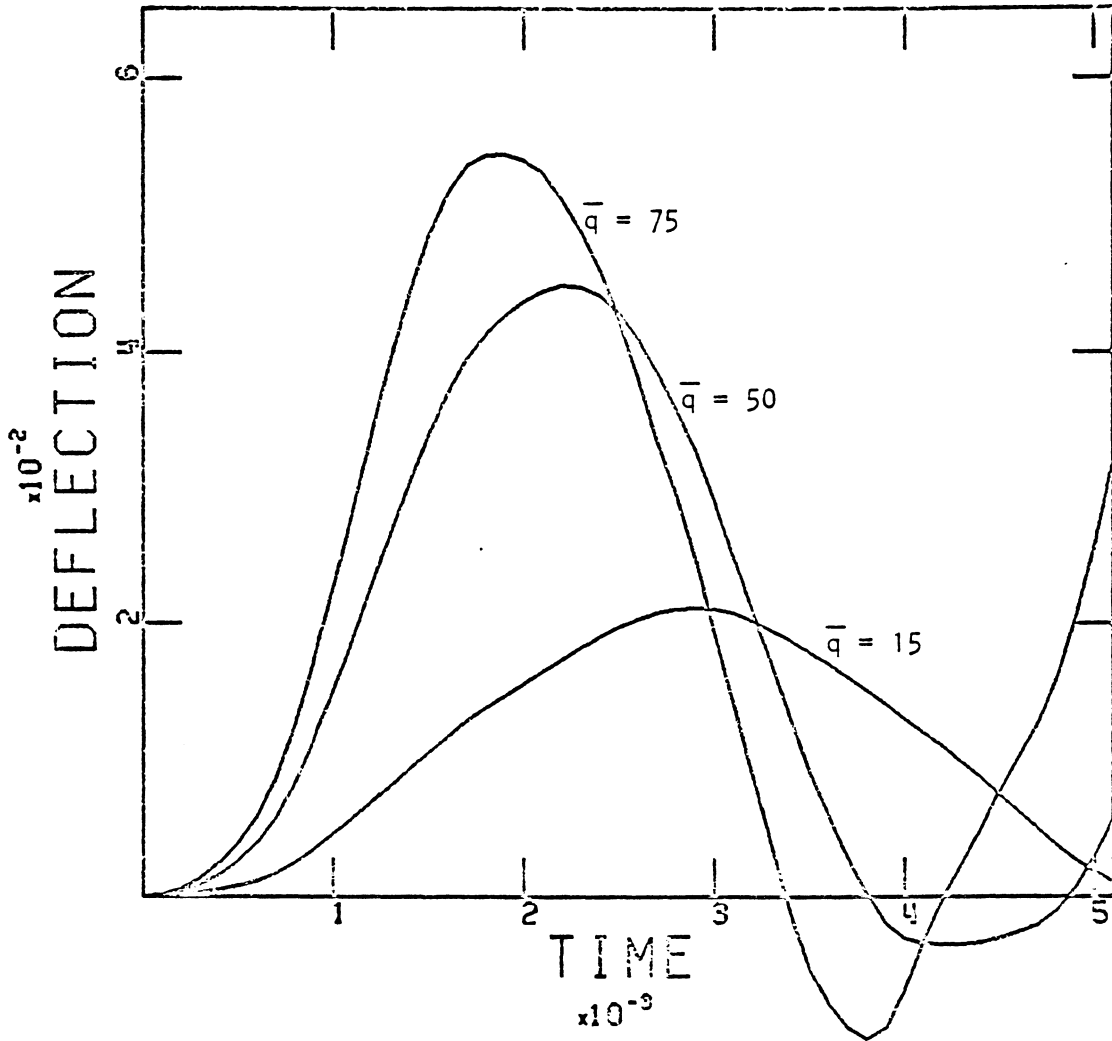


Figure 13 Effect of Load Magnitude.

Note the nonlinear effect.

As the deflection increases,

the stiffness also increases

due to the midplane stretching.

EFFECT OF ORTHOTROPY - $E_1/E_2 = 10, 25, 40$
 TWO-LAYER CROSS-PLY, UDL, SS, SQ. PLATE WITH $A/H=10$
 $Q_{BAR}=50, G_{12}=G_{13}=G_{23}=E_2/2$

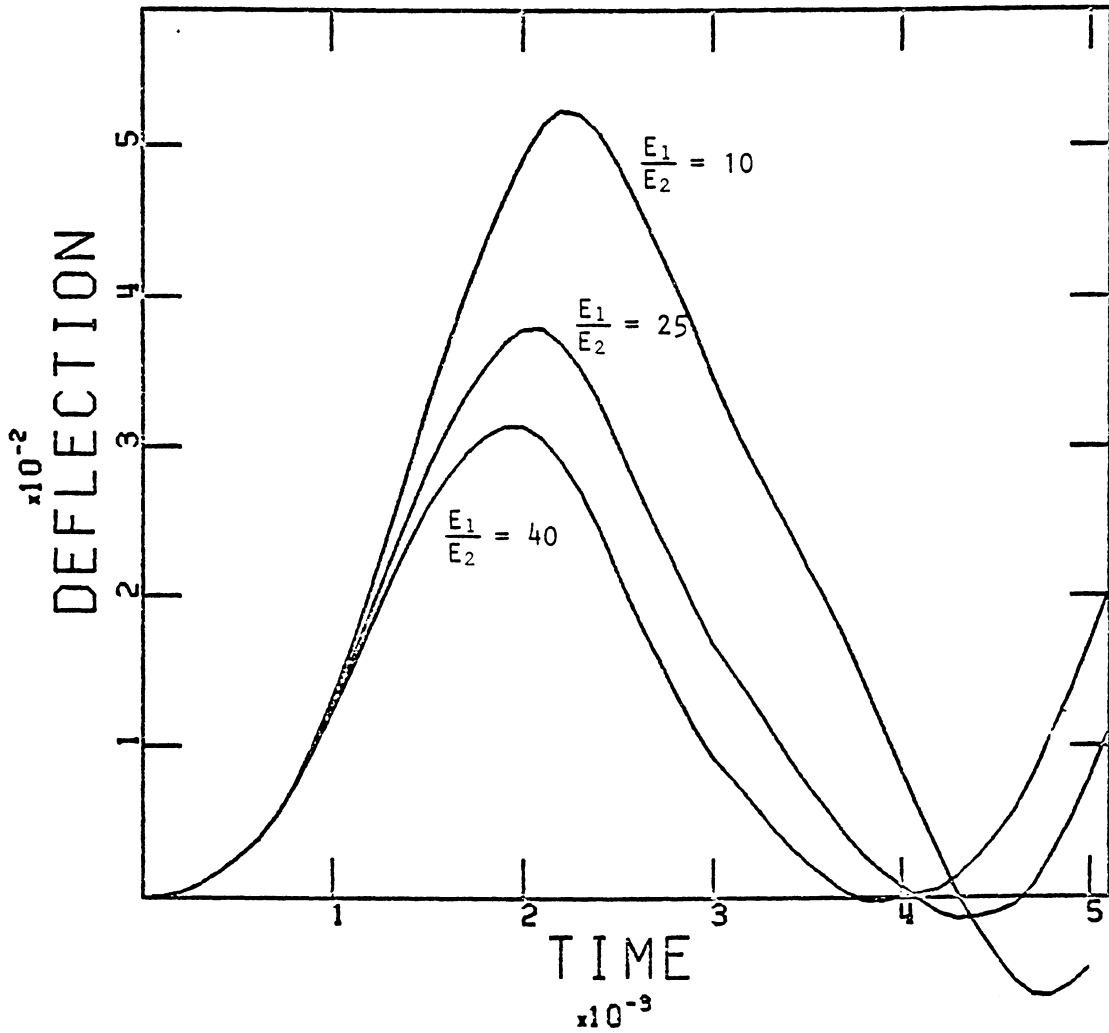


Figure 14 Effect of Orthotropy.

Increasing E_1 while holding the other plate properties constant produces a plate which is more resistant to bending.

EFFECT OF PLATE ASPECT RATIO - $A/B = 1.0, 1.5, 2.0$
 TWO-LAYER CROSS-PLY, UDL, SS, SQ. PLATE WITH $A/H=10$
 $QBAR=50, E1/E2=25$

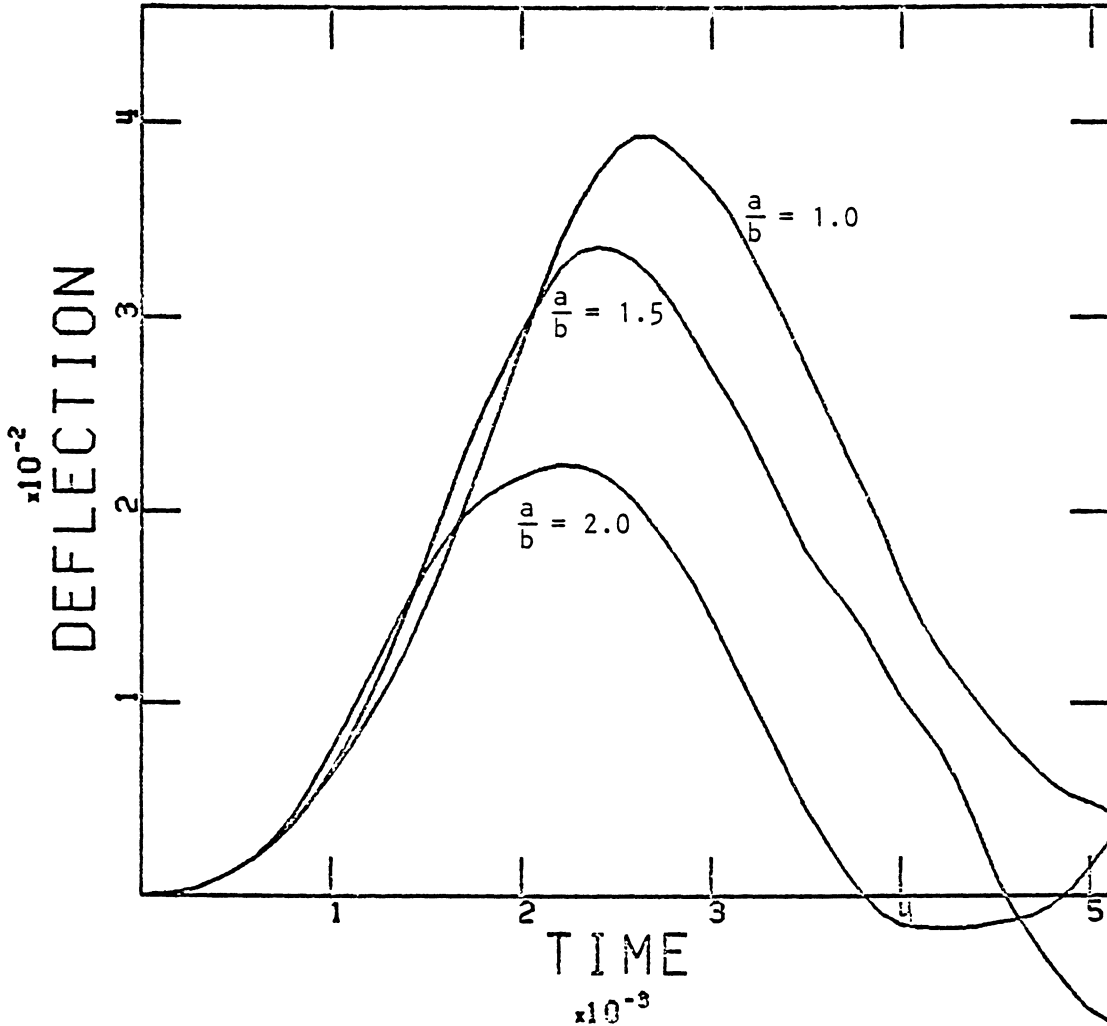


Figure 15 Effect of Plate Aspect Ratio.

The plate is stiffer for lower
 a/b ratios.

Cross-ply plates do not account for coupling between the in-plane shear and normal stresses and strains. For example, the stress-strain relations for a single layer in plane stress may be written

$$\begin{Bmatrix} \sigma_x \\ \sigma_y \\ \tau_{xy} \end{Bmatrix} = \begin{bmatrix} \bar{Q}_{11} & \bar{Q}_{12} & \bar{Q}_{16} \\ & \bar{Q}_{22} & \bar{Q}_{26} \\ & & \bar{Q}_{66} \end{bmatrix} \begin{Bmatrix} \epsilon_x \\ \epsilon_y \\ \gamma_{xy} \end{Bmatrix} \quad (4.4.2)$$

Note that the $[Q]$ matrix should not be confused with the normalized load magnitude, \bar{q} . The expressions for Q_{16} and Q_{26} are

$$\begin{aligned} \bar{Q}_{16} &= m^3 n (Q_{11} - Q_{12} - 2Q_{66}) + mn^3 (Q_{12} - Q_{22} + 2Q_{66}) \\ \bar{Q}_{26} &= mn^3 (Q_{11} - Q_{12} - 2Q_{66}) + m^3 n (Q_{12} - Q_{22} + 2Q_{66}) \end{aligned} \quad (4.4.3)$$

For a cross-ply laminate ($0^\circ/90^\circ$), Q_{16} and Q_{26} are zero, effectively uncoupling the shear quantities from the normal quantities. Thus, the plate exhibits less bending stiffness and shows a greater deflection for a given load magnitude (see Figure 16). Although eqn. (4.3.1) strictly applies only to plane stress within a layer, the uncoupling phenomenon occurs in the general case.

In Figure (17), the effect of plate thickness is plotted. Note that the thin plate has a much higher peak deflection than the thick plate for the same normalized load magnitude \bar{q} . This is another indication of the effect of transverse shear and geometric nonlinearities, which are much more pronounced in thick plates than in thin. The effect of including geometric nonlinearities is to increase the bending resistance in thick-plate or large deflection analysis. Figure (17) has

EFFECT OF LAMINATION SCHEME - CP, AP=5,15,25,35,45
 TWO-LAYER CROSS-PLY, UDL, SS, SQ. PLATE WITH A/H=10
 QBAR=50, E1/E2=25

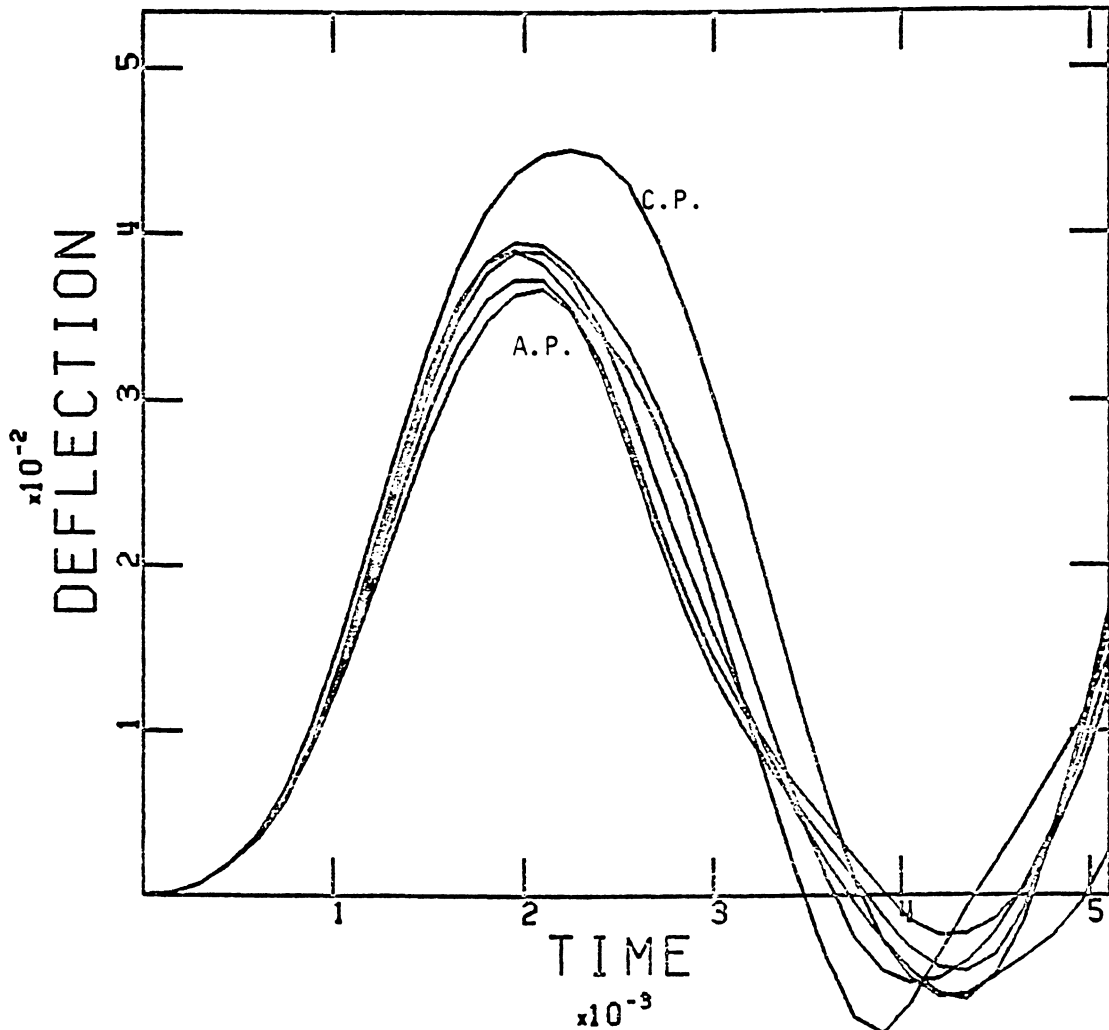


Figure 16 Effect of Lamination Scheme.

The A.P. plates are $\pm 5^\circ$, $\pm 15^\circ$, $\pm 25^\circ$, $\pm 35^\circ$, $\pm 45^\circ$. All A.P. plates showed greater greater stiffness than the C.P. plate. This may be attributed to the \bar{Q}_{16} , \bar{Q}_{26} terms as discussed on page 46.

the normalized deflection plotted for identical normalized loads, and clearly the thick plate exhibits much greater bending stiffness than the thin plate. The thick plate has a higher frequency and a lower peak deflection.

The effects of boundary conditions, Newmark parameters α and β , and time-step size were previously discussed in Chapter III and will not be repeated here.

EFFECT OF PLATE THICKNESS - $(A,B)/H = 10, 20$
 TWO-LAYER CROSS-PLY, UDL, SS, SQ. PLATE WITH $A/H=10$
 $QBAR=50, E1/E2=25$

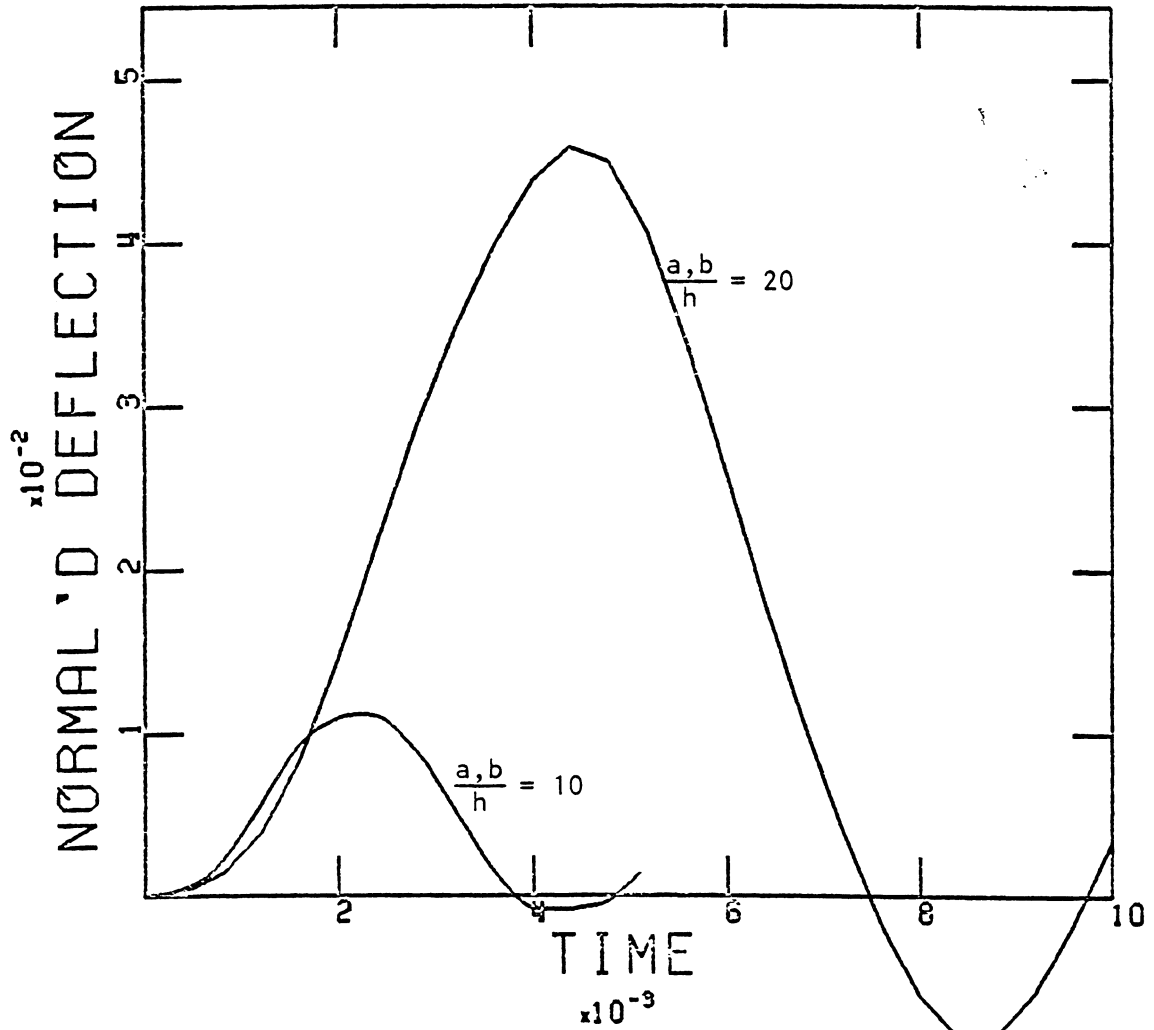


Figure 17 Effect of Plate Thickness.

The normalized deflection is much less for the thick plate because of nonlinear effects, transverse shear deformation, and rotatory inertia. The thick plate exhibits much greater stiffness than the thin plate.

Chapter V

SUMMARY AND CONCLUSIONS

5.1 SUMMARY

In the introductory chapter, the effects of transverse shear deformation and geometric nonlinearities were shown to be potentially significant in the bending response of laminated anisotropic plates. In the results presented throughout the thesis, this significance was proven for a number of specific cases. These effects are especially pronounced for large deflections, thick plates, or plates with high ratios of the in-plane Young's modulus to the transverse shear modulus.

Classical theory has proven to be inadequate in predicting the bending response of such plates because the theory ignores transverse shear deformation and geometric nonlinearity. Numerous alternate theories have been proposed suggesting several different methods of accounting for these effects. In this thesis, a theory due to Yang, Norris, and Stavsky was used to account for transverse shear deformation and rotatory inertia. The von Karman assumptions were used to account for geometric nonlinearities, and Newmark's direct integration technique was employed to integrate the resulting equations of motion.

Next, a computer program was developed which incorporates the theory and approximations as outlined in the text. The program is simple to use and has general applications for analysis work. Other

analysts could use the program in its present form to solve a range of problems. Such capabilities as accounting for material nonlinearities can be added (in this case, to the STIFF subroutine) without much difficulty, and without disturbing the execution logic.

The program was used to analyze the effects of load magnitude, material orthotropy, plate aspect ratio, plate thickness, and lamination scheme on the bending response of two-layer unsymmetric laminated plates.

5.2 CONCLUSIONS

The method developed in this thesis (also reported in <10>) gives excellent results in the transient bending analysis of laminated composite plates. The computer program is accurate, efficient, and general, and apparently represents the first transient finite-element analysis of laminated composite plate bending which accounts for transverse shear, rotatory inertia, and geometric nonlinearities. These effects may give solutions which differ significantly from the classical solutions, as shown in Chapter IV. Thus, this program will be valuable in analysis work. The benefits are especially useful when analyzing thick-plate response, large deflections, or materials with a high ratio of the in-plane Young's modulus to the transverse shear modulus. Many problems of practical importance fall into one or more of these categories.

Although the program is currently written for transversely isotropic materials with constant material properties, it may be easily

adapted to more anisotropic materials or to materials with material nonlinearities. This is accomplished by modifying the stiffness subroutine. The basic program logic which assembles and solves the global equations is not affected by the type of element used.

Finally, to reiterate, the program developed in this thesis works well and represents the first transient finite-element analysis of laminated composite plate bending which accounts for transverse shear deformation, rotatory inertia, and geometric nonlinearities.

REFERENCES

1. Yang, P. C., Norris, C. H., and Stavsky, Y. 'Elastic Wave Propagation in Heterogeneous Plates', *International Journal of Solids and Structures*, Vol. 2, 1966, pp. 665-684.
2. Reissner, E. 'The Effect of Transverse Shear Deformation on the Bending of Elastic Plates,' *Journal of Applied Mechanics*, Vol. 12, No. 2, Trans. ASME, Vol. 67, June 1945, pp. 69-77.
3. Mindlin, R. D. 'Influence of Rotatory Inertia and Shear on Flexural Motions of Isotropic, Elastic Plates,' *Journal of Applied Mechanics*, Vol. 18, No. 1, Trans. ASME, Vol. 73, Mar. 1951, pp.31-38
4. Stavsky, Y. 'On the Theory of Symmetrically Heterogeneous Plates Having the Same Thickness Variation of the Elastic Moduli', *Topics in Applied Mechanics*, Ed. by Abir, D., Ollendorff, F. and Reiner, M., American Elsevier, New York, 1965.
5. Ambartsumyan, S. A. *Theory of Anisotropic Plates* translated from Russian by Cheron, T., and ed. Ashton, J. E., Technomic, 1969.
6. Pryor, Jr., C. W., and Barker, R. M. 'A Finite Element Analysis Including Transverse Shear Effects for Applications to Laminated Plates', *AIAA Journal*, Vol. 9, pp. 912-917, 1971.
7. Noor, A. K. and Hartley, S. J. 'Effect of Shear Deformation and Anisotropy on the Non-Linear Response of Composite Plates', *Developments in Composite Materials - 1*, Ed. Holister, G., Applied Science Publishers, Barking, Essex, England, pp. 55-65, 1977.
8. Reddy, J. N. 'A Penalty Plate-Bending Element for the Analysis of Laminated Anisotropic Composite Plates', *Int. J. Numer. Meth. Engng.*, Vol. 15, pp. 1187-1206, 1980.
9. Reddy, J. N. and Chao, W. C. 'Nonlinear Bending of Thick Rectangular, Laminated Composite Plates', *Int. J. Nonlinear Mechanics*, 1981, to appear.
10. Reddy, J. N. and Mook, D. J. 'Transient Analysis of Layered Composite Plates Using A Shear Deformation Theory', to be presented at the Int'l. Conf. on Computational Methods and Experimental Measurements, Washington, D.C., June 30-July 2, 1982.
11. Volterra, E. and Zachmanoglou, E. C. *Dynamics of Vibrations*, Merrill, Columbus, Ohio, 1965.

12. Reismann, H. and Lee, Y. 'Forced Motions of Rectangular Plates', *Developments in Theoretical and Applied Mechanics*, Vol. 4, D. Frederick (ed.), pp. 3-18, Pergamon Press, New York, 1969.
13. Akay, H. U. 'Dynamic Large Deflection Analysis of Plates Using Mixed Finite Elements', *Computers and Structures*, Vol. 11, pp. 1-11, Pergamon Press, 1980.
14. Jones, Robert M. *Mechanics of Composite Materials*, Scripta Book Company (McGraw-Hill), Washington, D.C., 1975.
15. Ashton, J. E., and Whitney, J. M. *Theory Of Laminated Plates*, TECHNOMIC Publishing Co., Stamford, CT, 1970.
16. Tsai, Steven W. *Mechanics of Composite Materials, Part II, Theoretical Aspects*, Air Force Materials Laboratory Tech. Report AFML-TR-66-149, November, 1966.
17. Whitney, J. M. and Pagano, N. J. 'Shear Deformation in Heterogeneous Anisotropic Plates', *J. Applied Mechanics*, Vol. 37, pp. 1031-1036, 1970.
18. Bathe, K. J. and Wilson, E. L. *Numerical Methods In Finite Element Analysis*, Prentice-Hall, Englewood Cliffs, New Jersey, 1976.

Appendix A

MASS AND STIFFNESS MATRICES IN PROGRAM

Stiffness Matrix

$$[K] = \begin{bmatrix} \tau[K^{11}] & \tau[K^{12}] & \lambda^2[K^{13}] & \mu[K^{14}] & \mu[K^{15}] \\ \tau[K^{21}] & \tau[K^{22}] & \lambda^2[K^{23}] & \mu[K^{24}] & \mu[K^{25}] \\ \lambda\tau[K^{31}] & \lambda\tau[K^{32}] & \lambda[K_1^{33}] & \mu[K_1^{34}] & \mu[K_1^{35}] \\ & & + \lambda^3[K_2^{33}] & + \mu\lambda[K_2^{34}] & + \mu\lambda[K_2^{35}] \\ \tau[K^{41}] & \tau[K^{42}] & \lambda[K_1^{43}] & \mu[K^{44}] & \mu[K^{45}] \\ & & + \lambda^2[K_2^{43}] & & \\ \tau[K^{51}] & \tau[K^{52}] & \lambda[K_1^{53}] & \mu[K^{54}] & \mu[K^{55}] \\ & & + \lambda^2[K_2^{53}] & & \end{bmatrix}$$

Mass Matrix

$$[M] = \begin{bmatrix} P[S] & [0] & [0] & R[S] & [0] \\ [0] & P[S] & [0] & [0] & R[S] \\ [0] & [0] & P[S] & [0] & [0] \\ R[S] & [0] & [0] & I[S] & [0] \\ [0] & R[S] & [0] & [0] & I[S] \end{bmatrix}$$

The matrix coefficients $K_{ij}^{\alpha\beta}$ are given by

$$[K^{11}] = A_{11}[S^{xx}] + A_{16}([S^{xy}] + [S^{xy}]^T) + A_{66}[S^{yy}],$$

$$[K^{12}] = A_{12}[S^{xy}] + A_{16}[S^{xx}] + A_{26}[S^{yy}] + A_{66}[S^{xy}]^T = [K^{21}]^T,$$

$$[K^{13}] = A_{11}[R_x^{xx}] + A_{12}[R_y^{xy}] + A_{16}([R_x^{xy}] + [R_x^{xy}]^T + [R_y^{xx}]) \\ + A_{26}[R_y^{yy}] + A_{66}([R_y^{xy}]^T + [R_x^{yy}]^T + [R_x^{yy}]) = \frac{1}{2} [K^{31}]^T,$$

$$[K^{14}] = B_{11}[S^{xx}] + B_{16}([S^{xy}] + [S^{xy}]^T) + B_{66}[S^{yy}] = [K^{41}]^T,$$

$$[K^{15}] = B_{12}[S^{XY}] + B_{16}([S^{XY}] + [S^{XY}]^T) + B_{26}[S^{YY}] + B_{66}[S^{XY}]^T = [K^{51}]^T,$$

$$[K^{22}] = A_{22}[S^{YY}] + A_{26}([S^{XY}]^T + [S^{XY}]) + A_{66}[S^{XX}],$$

$$[K^{23}] = A_{12}[R_X^{XY}]^T + A_{22}[R_Y^{YY}] + A_{26}([R_Y^{XY}]^T + [R_Y^{XY}] + [R_X^Y]) \\ + A_{16}[R_X^{XX}] + A_{66}([R_X^{XY}] + [R_Y^{XX}]) = \frac{1}{2} [K^{32}]$$

$$[K^{24}] = B_{12}[S^{XY}]^T + B_{26}[S^{YY}] + B_{16}[S^{XX}] + B_{66}[S^{XY}] = [K^{42}]^T,$$

$$[K^{25}] = B_{22}[S^{YY}] + B_{26}([S^{XY}] + [S^{XY}]^T) + B_{66}[S^{XX}] = [K^{52}]^T,$$

$$[K_1^{33}] = A_{55}[S^{XX}] + A_{45}([S^{XY}] + [S^{XY}]^T) + A_{44}[S^{YY}],$$

$$[K_2^{33}] = \frac{1}{2} \int_R e^{[\bar{N}_1 \frac{\partial \phi_i}{\partial x} \frac{\partial \phi_j}{\partial x} + \bar{N}_6 (\frac{\partial \phi_i}{\partial x} \frac{\partial \phi_j}{\partial x}) + \bar{N}_2 \frac{\partial \phi_i}{\partial y} \frac{\partial \phi_j}{\partial y}]} dx dy,$$

$$[K_1^{34}] = A_{55}[S^{XO}] + A_{45}[S^{YO}] = [K_1^{43}]^T,$$

$$[K_2^{34}] = B_{11}[R_X^{XX}] + B_{16}([R_X^{XY}] + [R_X^{XY}]^T + [R_Y^{XX}]) + B_{12}[R_Y^{XY}]^T \\ + B_{26}[R_Y^{YY}] + B_{66}([R_X^{YY}] + [R_Y^{XY}]) = 2[K_2^{43}]^T,$$

$$[K_1^{35}] = A_{45}[S^{XO}] + A_{44}[S^{YO}] = [K_1^{53}]^T,$$

$$[K_2^{35}] = B_{12}[R_X^{XY}] + B_{16}[R_X^{XX}] + B_{22}[R_Y^{YY}] + B_{26}([R_Y^{XY}]^T + [R_X^{YY}] \\ + [R_Y^{XY}]) + B_{66}([R_X^{XY}]^T + [R_Y^{XX}])$$

$$[K^{44}] = D_{11}[S^{XX}] + D_{16}[S^{XY}] + [S^{XY}]^T + D_{66}[S^{YY}] + A_{55}[S],$$

$$[K^{45}] = D_{12}[S^{XY}] + D_{16}[S^{XX}] + D_{26}[S^{YY}] + D_{66}[S^{XY}]^T + A_{45}[S] = [K^{54}]^T,$$

$$[K^{55}] = D_{26}([S^{XY}] + [S^{XY}]^T) + D_{66}[S^{XX}] + D_{22}[S^{YY}] + A_{44}[S].$$

and

$$S_{ij} = \int_{R^e} \frac{\partial \phi_i}{\partial \xi} \frac{\partial \phi_j}{\partial \eta} dx dy, \quad \epsilon, \eta = 0, x, y, \quad S_{ij}^{\infty} \equiv S_{ij},$$

$$R_{\zeta}^{\epsilon \eta} = \int_{R^e} \frac{1}{2} \left(\frac{\partial w}{\partial \zeta} \right) \frac{\partial \phi_i}{\partial \xi} \frac{\partial \phi_j}{\partial \eta} dx dy, \quad \zeta, \xi, \eta = 0, x, y,$$

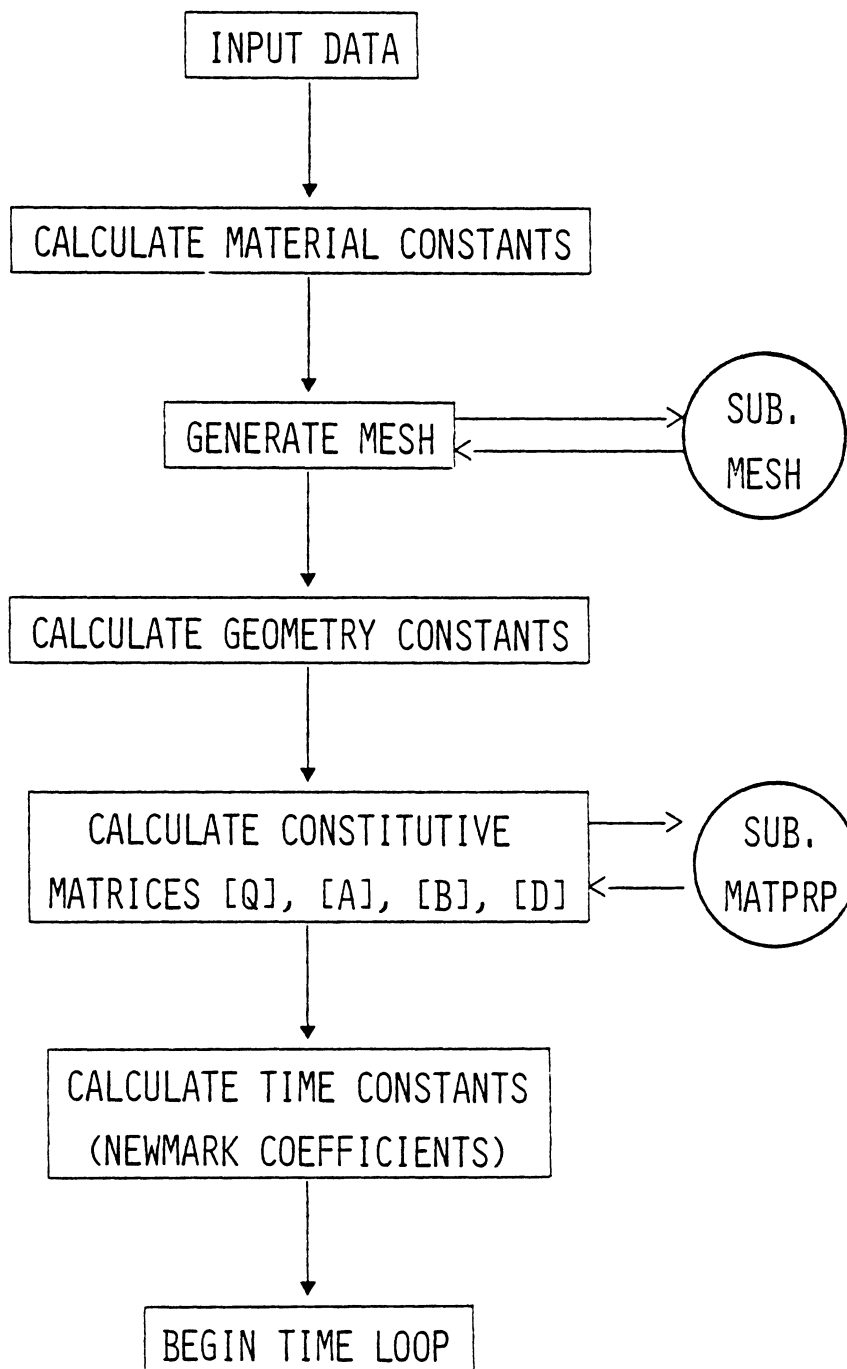
$$\bar{N}_1 = A_{11} \left(\frac{\partial w}{\partial x} \right)^2 + A_{12} \left(\frac{\partial w}{\partial y} \right)^2 + 2A_{16} \frac{\partial w}{\partial x} \frac{\partial w}{\partial y},$$

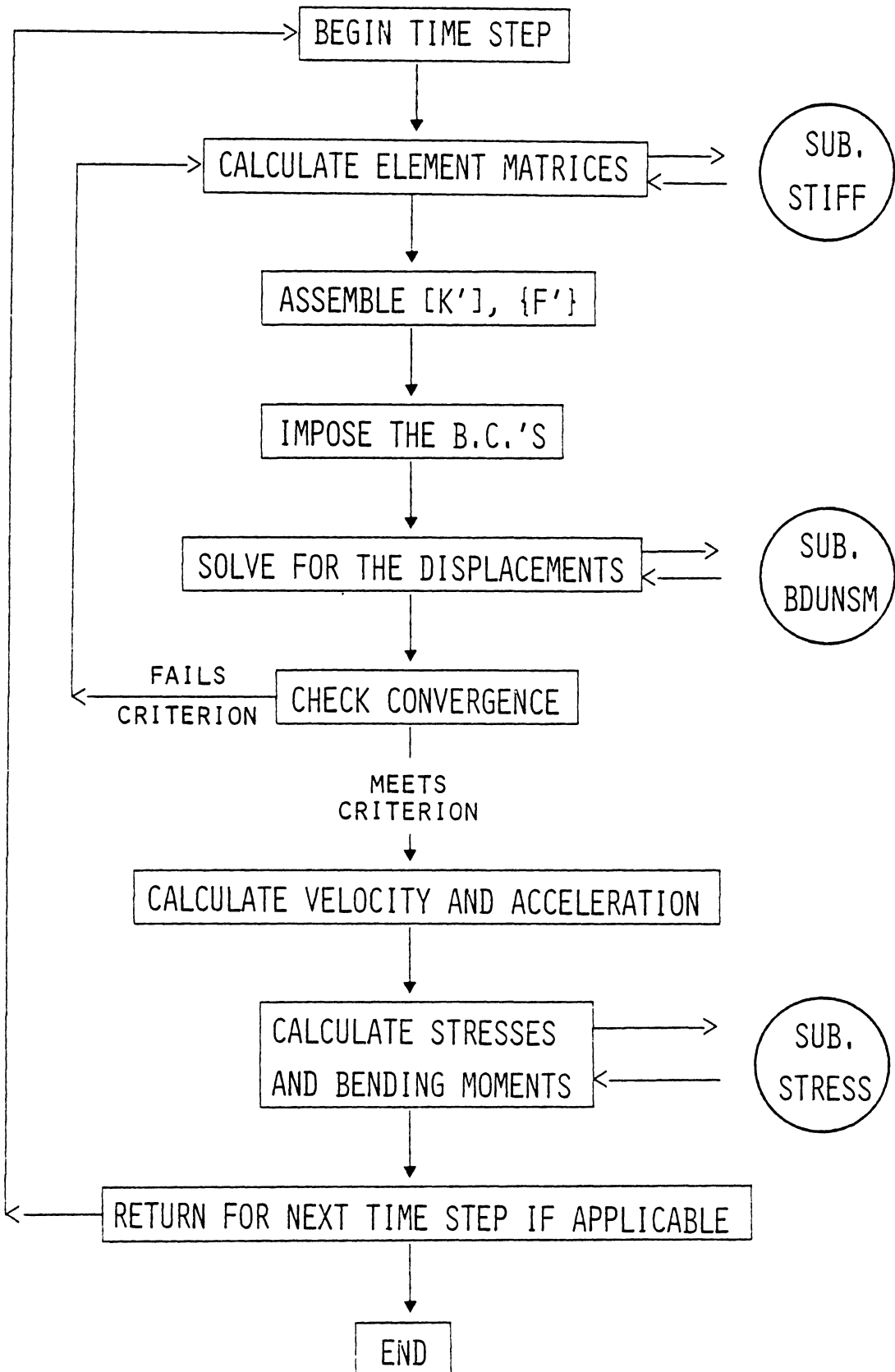
$$\bar{N}_2 = A_{12} \left(\frac{\partial w}{\partial x} \right)^2 + A_{22} \left(\frac{\partial w}{\partial y} \right)^2 + 2A_{26} \frac{\partial w}{\partial x} \frac{\partial w}{\partial y},$$

$$\bar{N}_6 = A_{16} \left(\frac{\partial w}{\partial x} \right)^2 + A_{26} \left(\frac{\partial w}{\partial y} \right)^2 + 2A_{66} \frac{\partial w}{\partial x} \frac{\partial w}{\partial y}.$$

Appendix B

FLOW DIAGRAM OF COMPUTER PROGRAM





Appendix C
LISTING OF COMPUTER PROGRAM

```

C *****MA|00010
C MA|00020
C PROGRAM FOR TRANSIENT ANALYSIS OF LAMINATED COMPOSITE PLATES MA|00030
C ACCOUNTING FOR TRANSVERSE SHEAR STRAINS AND GEOMETRIC NONLINEARITIESMA|00040
C MA|00050
C ORIGINAL VERSION DEVELOPED BY J.N. REDDY MA|00060
C MA|00070
C REVISED BY D.J. MOOK MA|00080
C MA|00090
C MA|00100
C QUANTITIES TO BE INPUT ARE AS FOLLOWS: MA|00110
C MA|00120
C CARD NO.  FORMAT  VARIABLES MA|00130
C MA|00140
C 1          615    LAYER; NO. OF LAYERS MA|00150
C                   NLS; NO. OF CASES (LOAD STEPS) TO BE RUN MA|00160
C                   INTER; SET EQUAL TO 1 MA|00170
C                   NPRNT; =1, CAUSES ELEMENT MATRICES TO BE PRINTEDMA|00180
C                   ILOAD; =0 FOR U.D.L MA|00190
C                   =1 FOR SINUSOIDAL QUARTER-PLATE LOADING MA|00200
C                   ITMAX; LIMIT ON NUMBER OF ITERATIONS AT ANY TIME MA|00210
C                   MA|00220
C 2          515    IEL; =1, LINEAR ELEMENT MA|00230
C                   =2, QUADRATIC ELEMENT MA|00240
C                   NDF; NUMBER OF DEGREES OF FREEDOM PER NODE MA|00250
C                   NPE; NODES PER ELEMENT MA|00260
C                   NRMAX; MAXIMUM ROW DIMENSION (= TOTAL D.O.F.) MA|00270
C                   NCMAX; MAXIMUM COLUMN DIMENSION (= BANDWIDTH) MA|00280
C                   MA|00290
C 3          1615   NTIME; INPUT 'NLS' TIMES - NUMBER OF TIME STEPS MA|00300
C                   MA|00310
C 4          215    IMESH; =1 FOR INPUT OF MESH INFORMATION; MA|00320
C                   OTHERWISE, AUTOMATIC MESH GENERATION MA|00330
C                   IVAL; =1, INPUT NONZERO BOUNDARY CONDITIONS MA|00340
C                   MA|00350
C 5          8F10   THETA; INPUT 'LAYER' TIMES - ANGLE OF EACH LAYERMA|00360
C                   MA|00370
C 6          8F10   H; TOTAL THICKNESS OF PLATE MA|00380
C                   DH; INPUT 'LAYER' TIMES - THICKNESS OF LAYER MA|00390
C                   MA|00400
C THE NEXT CARD IS INPUT FOR AUTOMATIC MESH GENERATION (IMESH NOT 1) MA|00410
C MA|00420
C (7) 215,2F10  NX; NUMBER OF ELEMENTS DESIRED IN X-DIRECTION MA|00430
C                   NY; NUMBER OF ELEMENTS DESIRED IN Y-DIRECTION MA|00440
C                   XL; LENGTH OF RECTANGLE IN X-DIRECTION MA|00450
C                   YL; LENGTH OF RECTANGLE IN Y-DIRECTION MA|00460
C                   MA|00470
C THE NEXT THREE (3) CARDS ARE INPUT IF 'IMESH' IS 1 MA|00480
C MA|00490
C (7) 215      NNODE; NUMBER OF NODES IN THE MESH MA|00500
C                   NEM; NUMBER OF ELEMENTS IN THE MESH MA|00510
C                   MA|00520

```

```

C      (8)      2F10      X; INPUT 'NNODE' TIMES - X-COORDINATES OF NODES MA100530
C      Y; INPUT 'NNODE' TIMES - Y-COORDINATES OF NODES MA100540
C      MA100550
C      (9)      1615      NOD(I,J); CONNECTIVITY MATRIX. NOD(I,J) MA100560
C      CONTAINS THE GLOBAL NUMBER OF NODE J MA100570
C      IN ELEMENT I. MA100580
C      MA100590
C      10      7F10      RHO; DENSITY OF THE MATERIAL MA100600
C      E1,E2; YOUNG'S MODULII IN MATERIAL COORDINATES MA100610
C      G12,G13,G23; SHEAR MODULII IN MATERIAL COORDS. MA100620
C      ANU12; POISSON'S RATIO IN MATERIAL COORDINATES MA100630
C      MA100640
C      11      8F10      DTM; INPUT 'NLS' TIMES - TIME-STEP SIZE MA100650
C      MA100660
C      12      8F10      PO; LOAD MAGNITUDE FOR INITIAL CASE MA100670
C      DP; INPUT 'NLS-1' TIMES - LOAD INCREMENT MA100680
C      MA100690
C      13      1F10      EPS; MAXIMUM ALLOWABLE ERROR FOR NONLINEAR ITER. MA100700
C      MA100710
C      14      3F10      ALFA; NEWMARK-BETA CONSTANTALPHA MA100720
C      GAMA; MA100730
C      AK; SHEAR CORRECTION COEFFICIENT MA100740
C      MA100750
C      15      15      NBDY; NUMBER OF BOUNDARY CONDITIONS MA100760
C      MA100770
C      THE NEXT CARD IS INPUT ONLY IF NBDY IS GREATER THAN ZERO MA100780
C      MA100790
C      (16)      1615      IBDY; INPUT 'NBDY' TIMES - IDENTIFIES NODAL B.C. MA100800
C      MA100810
C      THE NEXT CARD IS INPUT ONLY IF IVAL IS 1 MA100820
C      MA100830
C      (17)      8F10      VBDY; INPUT 'NBDY' TIMES - VALUE OF B.C. IBDY MA100840
C      MA100850
C      MA100860
C      IMPLICIT REAL*8(A-H,O-Z) MA100870
C      REAL*4 PT(52),DFL(52),PSTRSX(52),PSTRXY(52) MA100880
C      DIMENSION GSTIF(125,130),GP(125),GF(125),GFO(125),GF1(125), MA100890
C      * GF2(125),DP(11),DTM(5),NTIME(5) MA100900
C      DIMENSION VBDY(47),IBDY(47),A(6,6),C(3,3),THETA(16),DH(5) MA100910
C      COMMON/STIF1/ELXY(9,2),STIF(45,45),ELP(45),W(45),WO(45),W1(45), MA100920
C      * W2(45),AO,A1,A2,A3,A4,C1,C2,XL,YL MA100930
C      COMMON /MAT/Q(16,3,3),Z(17),Q44(16),Q45(16),Q55(16) MA100940
C      COMMON /MES1/X(81),Y(81),NOD(16,9) MA100950
C      READ(5,1000) LAYER,NLS,INTER,NPRNT,ILOAD,ITMAX MA100960
C      READ(5,1000) IEL,NDF,NPE,NRMAX,NCMAX MA100970
C      READ(5,1000) (NTIME(I),I=1,NLS) MA100980
C      READ(5,1000) IMESH,IVAL MA100990
C      READ(5,1001) (THETA(I),I=1,LAYER) MA101000
C      READ(5,1001) H,(DH(I),I=1,LAYER) MA101010
C      IF(IMESH.EQ.1) GO TO 1 MA101020
C      READ(5,1002) NX,NY,XL,YL MA101030
C      GO TO 2 MA101040
C      1 READ(5,1000) NNODE,NEM MA101050
C      READ(5,1001) (X(I),Y(I),I=1,NNODE) MA101060
C      READ(5,1000) ((NOD(I,J),J=1,NPE),I=1,NEM) MA101070
C      2 READ(5,1001) RHO,E1,E2,G12,G13,G23,ANU12

```

```

READ(5,1001) (DTM(I), I=1,NLS) MA101080
READ(5,1001) PO,(DP(I), I=1,NLS) MA101090
READ(5,1001) EPS MA101100
READ(5,1001) ALFA,GAMA,AK MA101110
READ(5,1000) NBDY MA101120
IF(NBDY.EQ.0) GO TO 4 MA101130
READ(5,1000) (IBDY(I), I=1,NBDY) MA101140
DO 3 I=1,NBDY MA101150
3 VBDY(I)=0.DO MA101160
IF(IVAL.EQ.1) READ(5,1001) (VBDY(I), I=1,NBDY) MA101170
4 NGP = IEL+1 MA101180
LGP = IEL MA101190
BETA=0.25*(0.5+ALFA)**2 MA101200
ANU21=ANU12*E2/E1 MA101210
ALMDA=1.0-ANU12*ANU21 MA101220
C MA101230
C ***** MA101240
C MA101250
C CALCULATE THE STIFFNESS MATRIX IN MATERIAL PRINCIPLE COORDINATES MA101260
C ***** MA101270
C MA101280
C MA101290
C C(1,1)=E1/ALMDA MA101300
C C(1,2)=ANU12*E2/ALMDA MA101310
C C(1,3)=0.0 MA101320
C C(2,2)=E2/ALMDA MA101330
C C(2,3)=0.0 MA101340
C C(3,3)=G12 MA101350
DO 20 I=1,3 MA101360
DO 20 J=1,3 MA101370
20 C(J,I)=C(I,J) MA101380
WRITE(6,370) E1,E2,G12,G13,G23,ANU12,AK,RHO MA101390
WRITE(6,460) IEL,NGP,LGP MA101400
CALL MESH (NX,NY,NPE,NDF,NNM,NEM,IEL,XL,YL) MA101410
C MA101420
C ***** MA101430
C MA101440
C CALL SUBROUTINE MESH FOR MESH GENERATION MA101450
C ***** MA101460
C MA101470
C MA101480
DO 30 I=1,NBDY MA101490
30 VBDY(I)=0.0 MA101500
NEQ=NNM*NDF MA101510
WRITE(6,420) NEM,NNM,NDF MA101520
NN=NPE*NDF MA101530
WRITE(6,360) NBDY MA101540
WRITE(6,270) (IBDY(I), I=1,NBDY) MA101550
WRITE(6,290) MA101560
DO 40 I=1,NEM MA101570
40 WRITE(6,270) I,(NOD(I,J),J=1,NPE) MA101580
WRITE(6,350) MA101590
WRITE(6,280) (X(I),Y(I), I=1,NNM) MA101600
C MA101610
C ***** MA101620

```

```

C
C CALCULATE THE BANDWIDTH, HALF-BW, NO. OF EQNS., ETC MAI01630
C ***** MAI01640
C ***** MAI01650
C ***** MAI01660
C ***** MAI01670
C NHBW=0 MAI01680
C DO 50 N=1,NEM MAI01690
C DO 50 I=1,NPE MAI01700
C DO 50 J=1,NPE MAI01710
C NW=( IABS(NOD(N,I)-NOD(N,J))+1)*NDF MAI01720
50 IF (NHBW.LT.NW) NHBW=NW MAI01730
C WRITE(6,430) NHBW MAI01740
C NBW=2*NHBW MAI01750
C DO 240 NH=1,1 MAI01760
C ***** MAI01770
C ***** MAI01780
C ***** MAI01790
C CALCULATE P AND I (ROTATORY INERTIA) MAI01800
C ***** MAI01810
C ***** MAI01820
C ***** MAI01830
C C1=RHO*H MAI01840
C C2=(H**3)*RHO/12. MAI01850
C WRITE(6,390) MAI01860
C WRITE(6,480) H,LAYER,(THETA(K),K=1,LAYER) MAI01870
C ***** MAI01880
C ***** MAI01890
C ***** MAI01900
C CALL SUBROUTINE MATPRP TO CALCULATE QBAR MATRIX, AND A,B,D MATRICES MAI01910
C ***** MAI01920
C ***** MAI01930
C ***** MAI01940
C CALL MATPRP (LAYER,C,A,H,THETA,AK,G13,G23,A44,A45,A55) MAI01950
C WRITE(6,390) MAI01960
C DO 230 NP=1,NLS MAI01970
C PBAR=(2.0*XL)**4*PO/E2/(H**4) MAI01980
C WRITE(6,340) NP,DP(NP),PO,PBAR MAI01990
C DT=DTM(NP) MAI02000
C DT2=DT*DT MAI02010
C A0=1.0/BETA/DT2 MAI02020
C A2=1.0/BETA/DT MAI02030
C A1=ALFA*A2 MAI02040
C A3=0.5/BETA-1.0 MAI02050
C A4=ALFA/BETA-1.0 MAI02060
C WRITE(6,540) ALFA,BETA,A0,A1,A2,A3,A4 MAI02070
C WRITE(6,571) MAI02080
C ***** MAI02090
C ***** MAI02100
C ***** MAI02110
C SET THE INITIAL CONDITIONS MAI02120
C ***** MAI02130
C ***** MAI02140
C ***** MAI02150
C ***** MAI02160
C ***** MAI02170
C DO 60 I=1,NEQ
C GF(I)=0.0

```

```

        GF0(I)=0.0
        GF1(I)=0.0
        GF2(I)=0.0
60     GSTIF(I,NBW)=0.0
        NSTART=1
        T=DT*(NSTART-1)
        NNTIME=NNTIME(NP)
        WRITE(11,1004) NNTIME,DT
1004  FORMAT(5X,'NUM. OF TIME STEPS =',I3,5X,'TIME STEP =',D12.4)
C *****
C
C     BEGIN TIME MARCH
C *****
C
C     DO 225 NT=NSTART,NNTIME
C     T=T+DT
C     ITER=0
70    ITER=ITER+1
C     IF (ITER.GT.ITMAX) GO TO 185
C     DO 80 I=1,NEQ
C     GP(I)=GF(I)
C     GF(I)=GSTIF(I,NBW)
C     DO 80 J=1,NBW
80    GSTIF(I,J)=0.0
C *****
C
C     BEGIN STIFFNESS MATRIX ITERATION FOR THIS TIME
C *****
C
C     DO 130 N=1,NEM
C     L=0
C     DO 90 I=1,NPE
C     NI=NOD(N,I)
C     ELXY(I,1)=X(NI)
C     ELXY(I,2)=Y(NI)
C     LI=(NI-1)*NDF
C     DO 90 J=1,NDF
C     LI=LI+1
C     L=L+1
C     W0(L)=GFO(LI)
C     W1(L)=GF1(LI)
C     W2(L)=GF2(LI)
C     W(L)=GAMA*GP(LI)+(1.0-GAMA)*GF(LI)
90    IF(ITMAX.EQ.1)W(L)=0.0
C *****
C
C     CALL SUBROUTINE STIFF TO CALCULATE THE ELEMENT MASS AND STIFFNESS
C     AND STIFFNESS MATRICES AND THE ELEMENT FORCE VECTOR
C
C     THE MODIFICATIONS FOR THE NEWMARK DIRECT INTEGRATION TECHNIQUE

```

```

MAI02180
MAI02190
MAI02200
MAI02210
MAI02220
MAI02230
MAI02240
MAI02250
MAI02260
MAI02270
MAI02280
MAI02290
MAI02300
MAI02310
MAI02320
MAI02330
MAI02340
MAI02350
MAI02360
MAI02370
MAI02380
MAI02390
MAI02400
MAI02410
MAI02420
MAI02430
MAI02440
MAI02450
MAI02460
MAI02470
MAI02480
MAI02490
MAI02500
MAI02510
MAI02520
MAI02530
MAI02540
MAI02550
MAI02560
MAI02570
MAI02580
MAI02590
MAI02600
MAI02610
MAI02620
MAI02630
MAI02640
MAI02650
MAI02660
MAI02670
MAI02680
MAI02690
MAI02700
MAI02710
MAI02720

```

```

C ARE CARRIED OUT AT THE ELEMENT LEVEL IN SUBROUTINE STIFF MA102730
C ***** MA102740
C ***** MA102750
C ***** MA102760
C CALL STIFF(NPE, NN, NGP, LGP, ILOAD, NT, A, A44, A45, A55, PO, ITER, N) MA102770
C IF (NPRNT.EQ.0) GO TO 110 MA102780
C IF (N.GT.1) GO TO 110 MA102790
C WRITE(6,320) MA102800
C DO 100 I=1, NN MA102810
100 WRITE(6,300) (STIF(I,J), J=1, NN) MA102820
C WRITE(6,310) MA102830
C WRITE(6,300) (ELP(I), I=1, NN) MA102840
C WRITE(6,310) MA102850
110 CONTINUE MA102860
C ***** MA102870
C ***** MA102880
C ***** MA102890
C ASSEMBLE THE ELEMENT STIFFNESS MATRICES TO GET THE GLOBAL MA102900
C STIFFNESS MATRIX AND THE ELEMENT FORCE VECTORS TO GET THE GLOBAL MA102910
C FORCE VECTOR. MA102920
C ***** MA102930
C ***** MA102940
C ***** MA102950
C DO 130 I=1, NPE MA102960
C NR=(NOD(N, I)-1)*NDF MA102970
C DO 130 II=1, NDF MA102980
C NR=NR+1 MA102990
C L=(I-1)*NDF+II MA103000
C GSTIF(NR, NBW)=GSTIF(NR, NBW)+ELP(L) MA103010
C DO 130 J=1, NPE MA103020
C NCL=(NOD(N, J)-1)*NDF MA103030
C DO 130 JJ=1, NDF MA103040
C M=(J-1)*NDF+JJ MA103050
C NC=NCL+JJ-NR+NHBW MA103060
C IF (NC) 130, 130, 120 MA103070
120 GSTIF(NR, NC)=GSTIF(NR, NC)+STIF(L, M) MA103080
130 CONTINUE MA103090
C ***** MA103100
C ***** MA103110
C ***** MA103120
C IMPOSE THE BOUNDARY CONDITIONS MA103130
C ***** MA103140
C ***** MA103150
C ***** MA103160
C N1=NDF-1 MA103170
C N2=NDF-2 MA103180
C IF (ILOAD.EQ.0) GSTIF(N2, NBW)=GSTIF(N2, NBW)+0.25*PO MA103190
C DO 150 I=1, NBDY MA103200
C IB=IBDY(I) MA103210
C VB=VBDY(I) MA103220
C DO 140 J=1, NBW MA103230
140 GSTIF(IB, J)=0.0 MA103240
C GSTIF(IB, NHBW)=1.0 MA103250
150 GSTIF(IB, NBW)=VB MA103260
C ***** MA103270

```

```

C *****MAI03280
C MAI03290
C CALL SUBROUTINE BDUNSM TO SOLVE THE SYSTEM OF SIMULTANEOUS
C EQUATIONS. THE SOLUTION (THE NODE-POINT DISPLACEMENTS) IS
C RETURNED IN THE LAST COLUMN OF THE COEFFICIENT MATRIX (THE
C ASSEMBLED, MODIFIED GLOBAL STIFFNESS MATRIX) MAI03310
C MAI03320
C MAI03330
C MAI03340
C *****MAI03350
C MAI03360
C CALL BDUNSM (GSTIF, NRMAX, NCMAX, NEQ, NHBW) MAI03370
C ERR=0.0 MAI03380
C IF (ITMAX.EQ.1) GO TO 180 MAI03390
C DO 170 I=N2, NEQ, NDF MAI03400
170 ERR=(GSTIF(I, NBW)-GF(I))**2+ERR MAI03410
C ERR=DSQRT(ERR)/DABS(GSTIF(N2, NBW)) MAI03420
C IF (ERR.GT.EPS) GO TO 70 MAI03430
C GOTO 185 MAI03440
180 WRITE(6,550) ITER MAI03450
185 CONTINUE MAI03460
C MAI03470
C *****MAI03480
C MAI03490
C CALCULATE THE VELOCITY AND ACCELERATION VECTORS USING THE DIS-
C PLACEMENT VECTOR AND EQNS. 3.4.1 FROM SECTION 3.4 MAI03500
C MAI03510
C MAI03520
C *****MAI03530
C MAI03540
C DO 65 I=1, NEQ MAI03550
C GF0(I)=A0*(GSTIF(I, NBW)-GF0(I))-A2*GF1(I)-A3*GF2(I) MAI03560
C GF1(I)=GF1(I)+DT*(1.0-ALFA)*GF2(I)+DT*ALFA*GF0(I) MAI03570
C GF2(I)=GF0(I) MAI03580
C GF0(I)=GSTIF(I, NBW) MAI03590
65 CONTINUE MAI03600
C IF(NPRNT.EQ.0)GOTO 195 MAI03610
C WRITE(6,560) MAI03620
C WRITE(6,530) NT,DT,T MAI03630
C IF (NDF.EQ.3) GO TO 190 MAI03640
C WRITE(6,380) MAI03650
C WRITE(6,300)(GSTIF(I, NBW), I=1, NEQ, NDF) MAI03660
C WRITE(6,310) MAI03670
C WRITE(6,300)(GF1(I), I=1, NEQ, NDF) MAI03680
C WRITE(6,310) MAI03690
C WRITE(6,300)(GF2(I), I=1, NEQ, NDF) MAI03700
C WRITE(6,440) MAI03710
C WRITE(6,300)(GSTIF(I, NBW), I=2, NEQ, NDF) MAI03720
C WRITE(6,310) MAI03730
C WRITE(6,300)(GF1(I), I=2, NEQ, NDF) MAI03740
C WRITE(6,310) MAI03750
C WRITE(6,300)(GF2(I), I=2, NEQ, NDF) MAI03760
190 WRITE(6,450) MAI03770
C WRITE(6,300)(GSTIF(I, NBW), I=N2, NEQ, NDF) MAI03780
C WRITE(6,310) MAI03790
C WRITE(6,300)(GF1(I), I=N2, NEQ, NDF) MAI03800
C WRITE(6,310) MAI03810
C WRITE(6,300)(GF2(I), I=N2, NEQ, NDF) MAI03820

```

```

WRITE(6,400)
WRITE(6,300)(GSTIF(I,NBW),I=N1,NEQ,NDF)
WRITE(6,310)
WRITE(6,300)(GF1(I),I=N1,NEQ,NDF)
WRITE(6,310)
WRITE(6,300)(GF2(I),I=N1,NEQ,NDF)
WRITE(6,410)
WRITE(6,300)(GSTIF(I,NBW),I=NDF,NEQ,NDF)
WRITE(6,310)
WRITE(6,300)(GF1(I),I=NDF,NEQ,NDF)
WRITE(6,310)
WRITE(6,300)(GF2(I),I=NDF,NEQ,NDF)
195 IF (ITMAX.EQ.1) GO TO 200
C *****
C IF THE SOLUTION AT THIS TIME STEP HAS NOT CONVERGED IN THE
C NUMBER OF ITERATIONS SPECIFIED IN THE INPUT, PROGRAM STOPS
C *****
C IF (ITER.GT.ITMAX) GO TO 250
C IF (ITER.EQ.1) GO TO 70
C WRITE(6,310)
200 CONTINUE
DO 220 N=1,NEM
L=0
DO 210 I=1,NPE
NI=NOD(N,I)
ELXY(I,1)=X(NI)
ELXY(I,2)=Y(NI)
LI=(NI-1)*NDF
DO 210 J=1,NDF
LI=LI+1
L=L+1
210 W(L)=GSTIF(LI,NBW)
C *****
C CALL SUBROUTINE STRESS TO CALCULATE THE 'SECONDARY' QUANTITIES
C SUCH AS STRESSES AND BENDING MOMENTS
C *****
C CALL STRESS (NPE,NDF,IEL,ELXY,W,LAYER,ITER,NP,STRSX,STRXY)
C IF(N.EQ.1)STRES=STRSX
220 CONTINUE
WRITE(6,570) T,GSTIF(N2,NBW),GF1(N2),GF2(N2),STRES,STRXY,ERR,ITER
PT(NT)=T
DFL(NT)=GF(N2)
PSTRSX(NT)=STRSX
PSTRXY(NT)=STRXY
DDFL=DFL(NT)
C *****
C *****

```

```

MA103830
MA103840
MA103850
MA103860
MA103870
MA103880
MA103890
MA103900
MA103910
MA103920
MA103930
MA103940
MA103950
MA103960
MA103970
MA103980
MA103990
MA104000
MA104010
MA104020
MA104030
MA104040
MA104050
MA104060
MA104070
MA104080
MA104090
MA104100
MA104110
MA104120
MA104130
MA104140
MA104150
MA104160
MA104170
MA104180
MA104190
MA104200
MA104210
MA104220
MA104230
MA104240
MA104250
MA104260
MA104270
MA104280
MA104290
MA104300
MA104310
MA104320
MA104330
MA104340
MA104350
MA104360
MA104370

```

```

C
C THE SOLUTION IS WRITTEN TO A TAPE FOR LATER USE (SUCH AS PLOTTING)
C *****
C
C WRITE(11,1003) PT(NT),DFL(NT),PSTRSX(NT),PSTRXY(NT)
225 CONTINUE
1003 FORMAT(6X,4E13.6)
      NTIME2=NTIME(NP)+2
      WRITE(6,390)
230 PO=PO+DP(NP)
240 CONTINUE
250 WRITE(6,330)
      STOP
C
270 FORMAT (16I5)
280 FORMAT (8F10.4)
290 FORMAT (/ ,4X, ' BOOLEAN (CONNECTIVITY) MATRIX-NOD(I,J) ',/)
300 FORMAT (8(2X,E12.5))
310 FORMAT (//)
320 FORMAT (/ , ' ELEMENT STIFFNESS MATRICES... ',/)
330 FORMAT (/ ,5X, '***** CONVERGENCE CRITERIA IS NOT SATISFIED ***** ',/
1)
340 FORMAT (/ ,5X, 'LOAD NUMBER = ',I3,5X, 'LOAD INCREMENT = ',E13.6,5X, 'LOMAI04610
1AD INTENSITY = ',E13.5,5X, 'LOAD PARM. = ',E13.5,/)
350 FORMAT (/ , ' COORDINATES OF THE GLOBAL NODES ',/)
360 FORMAT(5X, 'NUMBER OF SPECIFIED DEGREES OF FREEDOM=',I5,/,5X, 'SPECIMAI04640
*FIED DEGREES OF FREEDOM FOLLOW:',/)
370 FORMAT(5X, 'M A T E R I A L P R O P E R T I E S:',/,10X, 'MODULUS, MAI04660
*E1=',E12.5,/,10X, 'MODULUS, E2=',E12.5,/,10X, 'SHEAR MODULI, G12,G13MAI04670
*AND G23=',3E12.5,/,10X, 'POISSONS RATIO, NU12=',E12.5,/,10X, 'SHEAR MAI04680
*CORRECTION COEFFICIENT, K=',E12.5,/,10X, 'MATERIAL DENSITY, RHO=', MAI04690
*E12.5,/)
380 FORMAT (5X, ' ..U-DISPLACEMENT VECTOR... ',/)
390 FORMAT (120(' '),//)
400 FORMAT (//,5X, ' ...SHEAR SLOPE, SI-X... ',/)
410 FORMAT (//,5X, ' ...SHEAR SLOPE, SI-Y... ',/)
420 FORMAT (10X, 'ACTUAL NUMBER OF ELEMENTS IN THE MESH = ',I3,/,10X, 'NUMAI04750
1MBER OF NODES IN THE MESH = ',I3,/,10X, 'DEGREES OF FREEDOM = ',I2,/)MAI04760
430 FORMAT (//, ' HALF BAND WIDTH OF GLOBAL STIFFNESS MATRIX = ',I5,/) MAI04770
440 FORMAT (5X, ' ..V-DISPLACEMENT VECTOR... ',/)
450 FORMAT (5X, ' ..W-DISPLACEMENT VECTOR... ',/)
460 FORMAT (/ ,5X, 'ELEMENT TYPE(1=LINEAR,2=QUADRATIC) = ',I2,10X, 'NGP=',MAI04800
11X,12,3X, 'LGP=',I1X,12,/)
470 FORMAT (///,2X, 'ITERATION NO = ',I2,5X, 'ERROR = ',E13.6,/)
480 FORMAT (5X, 'THICKNESS = ',E10.3,2X, 'NUMBER OF LAYERS AND THEIR ORIEMAI04830
1NTATION = ',I3,///,5X,12E10.3,/)
490 FORMAT (/ ,5X,120(' '))
500 FORMAT (/ ,3X, 'STRESSES IN EACH LAYER, GAUSS POINT AND ELEMENT',/) MAI04860
510 FORMAT (/ ,10X, 'E L E M E N T N U M B E R = ',I3,/) MAI04870
520 FORMAT(8X, 'SIGMAXT',5X, 'SIGMAXB',5X, 'SIGMAYT',5X, 'SIGMAYB',5X, 'SIGMAI04880
1MXYT',5X, 'SIGMXYB',6X, 'TAUXZ ',6X, 'TAUYZ',5X, 'SX(MEMB)',5X, 'SY(MEMAI04890
2MB)')
530 FORMAT(//,5X, 'TIME NUMBER=',I3,5X, 'TIME STEP=',E12.5,5X, 'TOTAL TIMMAI04910
*E=',E12.5,/)

```

```

540 FORMAT(//,5X,'ALFA=',F8.4,5X,'BETA=',F8.4,5X,'A0,A1,...=',5E9.2,/)MA104930
550 FORMAT(//,5X,'ITERATION NO.=',I2,5X,'*** LINEAR SOLUTION ***',//)MA104940
560 FORMAT(/,10X,'**** CONVERGED NONLINEAR SOLUTION ****',/)MA104950
570 FORMAT(10X,7E13.5,13)MA104960
571 FORMAT(17X,'T',6X,'GSTIF(N2,NBW)',3X,'GF1(N2)',6X,'GF2(N2)',7X,
1 'STRES',8X,'STRXY',9X,'ERR',9X,'ITER',/)MA104980
1000 FORMAT(16I5)MA104990
1001 FORMAT(8D10.3)MA105000
1002 FORMAT(2I5,2D10.3)MA105010
ENDMA105020
CSTI00010
C *****STI00020
CSTI00030
C SUBROUTINE STIFF CALCULATES THE ELEMENT STIFFNESS AND MASSSTI00040
C MATRICES AND THE ELEMENT FORCE VECTOR. GEOMETRIC NONLINEARITIESSTI00050
C AND TRANSVERSE SHEAR DEFORMATION ARE INCLUDED IN THE CALCULATIONS.STI00060
C THE ELEMENTS AVAILABLE ARE FOUR, FIVE, OR NINE-NODED ISOPARAMETRICSTI00070
C ELEMENTS WITH EITHER THREE (W,SX,SY) OR FIVE (U,V,W,SX,SY) D.O.F.STI00080
CSTI00090
C THE MODIFICATIONS FOR THE NEWMARK DIRECT INTEGRATION TECHNIQUESTI00100
C ARE CARRIED OUT AT THE ELEMENT LEVEL AND THE MODIFIED STIFFNESSSTI00110
C MATRIX AND MODIFIED FORCE VECTOR ARE ASSEMBLED IN THE MAIN PROGRAMSTI00120
CSTI00130
C *****STI00140
CSTI00150
C SUBROUTINE STIFF(NPE,NN,NGP,LGP,ILOAD,NT,A,A44,A45,A55,PO,IT,N)STI00160
C IMPLICIT REAL*8(A-H,O-Z)STI00170
C COMMON/STIF1/ELXY(9,2),STIF(45,45),ELP(45),W(45),W0(45),W1(45),STI00180
C * W2(45),A0,A1,A2,A3,A4,C1,C2,XL,YLSTI00190
C COMMON/SHP/SF(9),GDSF(2,9)STI00200
C DIMENSION GAUSS(4,4),WT(4,4),A(6,6),H(45,45),STFL(16,45,45)STI00210
CSTI00220
C *****STI00230
CSTI00240
C THE DATA FOR GAUSS NUMERICAL INTEGRATION IS SPECIFIED HERESTI00250
CSTI00260
C *****STI00270
CSTI00280
C DATA GAUSS/4*0.000,-.57735027D0,.57735027D0,2*0.000,-.77459667D0,0STI00290
C 1.000,.77459667D0,0.000,-.86113631D0,-.33998104D0,.33998104D0,.8611STI00300
C 23631D0/STI00310
C DATA WT/2.000,3*0.000,2*1.000,2*0.000,.55555555D0,.88888888D0,.555STI00320
C 155555D0,0.000,.34785485D0,2*.65214515D0,.34785485D0/STI00330
C PI=3.141592650D0STI00340
C NDF=NN/NPESTI00350
C DO 10 I=1,NNSTI00360
C ELP(I)=0.0STI00370
C DO 10 J=1,NNSTI00380
C H(I,J)=0.0STI00390
10 STIF(I,J)=0.0STI00400
C N1=NDF-1STI00410
C N2=NDF-2STI00420
C N3=NDF-3STI00430
C DO 80 NI=1,NGPSTI00440
C DO 80 NJ=1,NGPSTI00450

```

```

          XI=GAUSS(NI,NGP)
          ETA=GAUSS(NJ,NGP)
C
C *****
C CALL SUBROUTINE SHAPE TO CALCULATE THE SHAPE FUNCTIONS, THEIR
C DERIVATIVES, AND THE JACOBIAN MATRIX
C *****
C CALL SHAPE (DET,ELXY,ETA,XI,NPE)
C CNST=DET*WT(NI,NGP)*WT(NJ,NGP)
C X=0.0
C Y=0.0
C FX=0.0
C FY=0.0
C DO 20 I=1,NPE
C X=X+SF(I)*ELXY(I,1)
C Y=Y+SF(I)*ELXY(I,2)
C 20 CONTINUE
C *****
C CALCULATE THE SINUSOIDAL LOAD ON THE QUARTER PLATE IF ILOAD = 2
C *****
C CX=PI*0.5/XL
C CY=PI*0.5/YL
C P=P0*DCOS(CX*X)*DCOS(CY*Y)
C *****
C CALCULATE THE UNIFORMLY DISTRIBUTED LOAD IF ILOAD IS NOT EQUAL TO 2
C *****
C IF (ILOAD.NE.2) P=P0
C DO 30 I=1,NPE
C L=(I-1)*NDF+1
C FX=FX+0.5*GDSF(1,I)*W(L+N3)
C FY=FY+0.5*GDSF(2,I)*W(L+N3)
C IF (ILOAD.EQ.0) GO TO 30
C ELP(L+N3)=ELP(L+N3)+CNST*SF(I)*P
C 30 CONTINUE
C I1=1
C DO 70 I=1,NPE
C JJ=1
C DO 60 J=1,NPE
C IF (NDF.EQ.3) GO TO 45
C H(I1,JJ)=H(I1,JJ) + C1*SF(I)*SF(J)*CNST
C H(I1+1,JJ+1)=H(I1+1,JJ+1) + C1*SF(I)*SF(J)*CNST
C IF (NT.GT.1 .OR. IT.GT.1)GOTO 40
C STIF(I1,JJ)=STIF(I1,JJ)+(GDSF(1,I)*(A(1,1)*GDSF(1,J)+A(1,3)*GDSF(2
C 1,J))+GDSF(2,I)*(A(1,3)*GDSF(1,J)+A(3,3)*GDSF(2,J)))*CNST

```

```

      STIF(II, JJ+1)=STIF(II, JJ+1)+(GDSF(1, I)*(A(1, 2)*GDSF(2, J)+A(1, 3)*GDSF(1, J))
1SF(1, J))+GDSF(2, I)*(A(3, 2)*GDSF(2, J)+A(3, 3)*GDSF(1, J))*CNST      STI01020
      STIF(II+1, JJ)=STIF(II+1, JJ)+(GDSF(1, J)*(A(1, 2)*GDSF(2, I)+A(1, 3)*GDSF(1, J))
1SF(1, I))+GDSF(2, J)*(A(3, 2)*GDSF(2, I)+A(3, 3)*GDSF(1, I))*CNST      STI01030
      STIF(II, JJ+N2)=STIF(II, JJ+N2)+(GDSF(1, I)*(A(1, 4)*GDSF(1, J)+A(1, 6)*GDSF(1, I))
1GDSF(2, J))+GDSF(2, I)*(A(3, 4)*GDSF(1, J)+A(3, 6)*GDSF(2, J))*CNST      STI01050
      STIF(II+N2, JJ)=STIF(II+N2, JJ)+(GDSF(1, J)*(A(1, 4)*GDSF(1, I)+A(1, 6)*GDSF(1, I))
1GDSF(2, I))+GDSF(2, J)*(A(3, 4)*GDSF(1, I)+A(3, 6)*GDSF(2, I))*CNST      STI01060
      STIF(II, JJ+N1)=STIF(II, JJ+N1)+(GDSF(1, I)*(A(1, 5)*GDSF(2, J)+A(1, 6)*GDSF(1, I))
1GDSF(1, J))+GDSF(2, I)*(A(3, 5)*GDSF(2, J)+A(3, 6)*GDSF(1, J))*CNST      STI01070
      STIF(II+N1, JJ)=STIF(II+N1, JJ)+(GDSF(1, J)*(A(1, 5)*GDSF(2, I)+A(1, 6)*GDSF(1, I))
1GDSF(1, I))+GDSF(2, J)*(A(3, 5)*GDSF(2, I)+A(3, 6)*GDSF(1, I))*CNST      STI01080
      STIF(II+1, JJ+1)=STIF(II+1, JJ+1)+(GDSF(1, I)*(A(3, 2)*GDSF(2, J)+A(3, 3)*GDSF(1, J))
1)*GDSF(1, J))+GDSF(2, I)*(A(2, 2)*GDSF(2, J)+A(2, 3)*GDSF(1, J))*CNST      STI01090
      STIF(II+1, JJ+N2)=STIF(II+1, JJ+N2)+(GDSF(1, I)*(A(3, 4)*GDSF(1, J)+A(3, 6)*GDSF(2, J))
1, 6)*GDSF(2, J))+GDSF(2, I)*(A(2, 4)*GDSF(1, J)+A(2, 6)*GDSF(2, J))*CNST      STI01100
      STIF(II+N2, JJ+1)=STIF(II+N2, JJ+1)+(GDSF(1, J)*(A(3, 4)*GDSF(1, I)+A(3, 6)*GDSF(1, I))
1, 6)*GDSF(2, I))+GDSF(2, J)*(A(2, 4)*GDSF(1, I)+A(2, 6)*GDSF(2, I))*CNST      STI01110
      STIF(II+1, JJ+N1)=STIF(II+1, JJ+N1)+(GDSF(1, I)*(A(3, 5)*GDSF(2, J)+A(3, 6)*GDSF(1, J))
1, 6)*GDSF(1, J))+GDSF(2, I)*(A(2, 5)*GDSF(2, J)+A(2, 6)*GDSF(1, J))*CNST      STI01120
      STIF(II+N1, JJ+1)=STIF(II+N1, JJ+1)+(GDSF(1, J)*(A(3, 5)*GDSF(2, I)+A(3, 6)*GDSF(1, I))
1, 6)*GDSF(1, I))+GDSF(2, J)*(A(2, 5)*GDSF(2, I)+A(2, 6)*GDSF(1, I))*CNST      STI01130
      GOTO 45      STI01230
C      STI01240
C *****      STI01250
C      STI01260
C      CALCULATE THE UNSYMMETRIC STIFFNESS COEFFICIENTS DUE TO THE      STI01270
C      GEOMETRIC NONLINEARITIES      STI01280
C      STI01290
C *****      STI01300
C      STI01310
C      40 CONTINUE      STI01320
      STIF(II, JJ+N3)=STIF(II, JJ+N3)+(GDSF(1, I)*(A(1, 1)*FX*GDSF(1, J)+A(1, 12)*FY*GDSF(2, J)
12)*FY*GDSF(2, J)+A(1, 3)*(FX*GDSF(2, J)+FY*GDSF(1, J))+GDSF(2, I)*(A(3, 2)*FX*GDSF(1, J)+A(3, 2)
2, 1)*FX*GDSF(1, J)+A(3, 2)*FY*GDSF(2, J)+A(3, 3)*(FX*GDSF(2, J)+FY*GDSF(3, 1, J)))*CNST      STI01330
      STIF(II+N3, JJ)=STIF(II+N3, JJ)+(GDSF(1, J)*(A(1, 1)*FX*GDSF(1, I)+A(1, 12)*FY*GDSF(2, I)+A(1, 3)
12)*FY*GDSF(2, I)+A(1, 3)*(FX*GDSF(2, I)+FY*GDSF(1, I))+GDSF(2, J)*(A(3, 2)*FX*GDSF(1, I)+A(3, 2)
2, 1)*FX*GDSF(1, I)+A(3, 2)*FY*GDSF(2, I)+A(3, 3)*(FX*GDSF(2, I)+FY*GDSF(3, 1, I)))*CNST*2.0      STI01340
      STIF(II+1, JJ+N3)=STIF(II+1, JJ+N3)+(GDSF(2, I)*(A(1, 2)*FX*GDSF(1, J)+A(1, 12)*FY*GDSF(2, J)
1A(2, 2)*FY*GDSF(2, J)+A(2, 3)*(FX*GDSF(2, J)+FY*GDSF(1, J))+GDSF(1, I)*(A(3, 2)*FX*GDSF(1, J)+A(3, 2)
2(A(1, 3)*FX*GDSF(1, J)+A(2, 3)*FY*GDSF(2, J)+A(3, 3)*(FX*GDSF(2, J)+FY*GDSF(3, 1, J)))*CNST      STI01350
      STIF(II+N3, JJ+1)=STIF(II+N3, JJ+1)+2.0*(GDSF(2, J)*(A(1, 2)*FX*GDSF(1, I)+A(1, 12)*FY*GDSF(2, I)
1, I)+A(2, 2)*FY*GDSF(2, I)+A(2, 3)*(FX*GDSF(2, I)+FY*GDSF(1, I))+GDSF(1, I)*(A(3, 2)*FX*GDSF(1, I)+A(3, 2)
2, J)*(A(1, 3)*FX*GDSF(1, I)+A(2, 3)*FY*GDSF(2, I)+A(3, 3)*(FX*GDSF(2, I)+FY*GDSF(3, 1, I)))*CNST      STI01360
      STI01370
      STI01380
      STI01390
      STI01400
      STI01410
      STI01420
      STI01430
      STI01440
      STI01450
      STI01460
      STI01470
      STI01480
      STI01490
C      STI01500
      45 IF(NT.GT.1 .OR. IT.GT.1)GOTO 50      STI01510
      STIF(II+N2, JJ+N2)=STIF(II+N2, JJ+N2)+(GDSF(1, I)*(A(4, 4)*GDSF(1, J)+A(4, 6)*GDSF(2, J))
1(4, 6)*GDSF(2, J))+GDSF(2, I)*(A(4, 6)*GDSF(1, J)+A(6, 6)*GDSF(2, J))*CNST      STI01520
      2ST      STI01530
      STIF(II+N2, JJ+N1)=STIF(II+N2, JJ+N1)+(GDSF(1, I)*(A(4, 5)*GDSF(2, J)+A(4, 6)*GDSF(1, J))
1(4, 6)*GDSF(1, J))+GDSF(2, I)*(A(5, 6)*GDSF(2, J)+A(6, 6)*GDSF(1, J))*CNST      STI01540
      STI01550

```

```

2ST
STIF(II+N1, JJ+N2)=STIF(II+N1, JJ+N2)+(GDSF(1, J)*(A(4, 5)*GDSF(2, I)+ASTI01570
1(4, 6)*GDSF(1, I))+GDSF(2, J)*(A(5, 6)*GDSF(2, I)+A(6, 6)*GDSF(1, I)))*CNSTI01580
2ST
STIF(II+N1, JJ+N1)=STIF(II+N1, JJ+N1)+(GDSF(1, I)*(A(5, 6)*GDSF(2, J)+ASTI01600
1(6, 6)*GDSF(1, J))+GDSF(2, I)*(A(5, 5)*GDSF(2, J)+A(5, 6)*GDSF(1, J)))*CNSTI01610
2ST
GOTO 55
C
50 CONTINUE
SW1=FX*GDSF(1, I)*(A(1, 1)*FX*GDSF(1, J)+A(1, 2)*FY*GDSF(2, J)+A(1, 3)*
1FX*GDSF(2, J)+FY*GDSF(1, J))+FY*GDSF(2, I)*(A(1, 2)*FX*GDSF(1, J)+A(2,
22)*FY*GDSF(2, J)+A(2, 3)*(FX*GDSF(2, J)+FY*GDSF(1, J)))
SW2=(FX*GDSF(2, I)+FY*GDSF(1, I))*(A(1, 3)*FX*GDSF(1, J)+A(2, 3)*FY*GDSSTI01690
1F(2, J)+A(3, 3)*(FX*GDSF(2, J)+FY*GDSF(1, J)))
STIF(II+N3, JJ+N3)=STIF(II+N3, JJ+N3)+2.0*(SW1+SW2)*CNST
STIF(II+N3, JJ+N2)=STIF(II+N3, JJ+N2)+2.0*(FX*GDSF(1, I)*(A(1, 4)*GDSFSTI01720
1(1, J)+A(1, 6)*GDSF(2, J))+FY*GDSF(2, I)*(A(2, 4)*GDSF(1, J)+A(2, 6)*GDSFSTI01730
2(2, J))+FY*GDSF(1, I)+FX*GDSF(2, I))*(A(3, 4)*GDSF(1, J)+A(3, 6)*GDSF(2STI01740
3, J))*CNST
STIF(II+N2, JJ+N3)=STIF(II+N2, JJ+N3)+(FX*GDSF(1, J)*(A(1, 4)*GDSF(1, I)STI01760
1)+A(1, 6)*GDSF(2, I))+FY*GDSF(2, J)*(A(2, 4)*GDSF(1, I)+A(2, 6)*GDSF(2, I)STI01770
2))+FY*GDSF(1, J)+FX*GDSF(2, J))*(A(3, 4)*GDSF(1, I)+A(3, 6)*GDSF(2, I))
3)*CNST
STIF(II+N3, JJ+N1)=STIF(II+N3, JJ+N1)+2.0*(FX*GDSF(1, I)*(A(1, 5)*GDSFSTI01800
1(2, J)+A(1, 6)*GDSF(1, J))+FY*GDSF(2, I)*(A(2, 5)*GDSF(2, J)+A(2, 6)*GDSFSTI01810
2(1, J))+FY*GDSF(1, I)+FX*GDSF(2, I))*(A(3, 5)*GDSF(2, J)+A(3, 6)*GDSF(1STI01820
3, J))*CNST
STIF(II+N1, JJ+N3)=STIF(II+N1, JJ+N3)+(FX*GDSF(1, J)*(A(1, 5)*GDSF(2, I)STI01840
1)+A(1, 6)*GDSF(1, I))+FY*GDSF(2, J)*(A(2, 5)*GDSF(2, I)+A(2, 6)*GDSF(1, I)STI01850
2))+FY*GDSF(1, J)+FX*GDSF(2, J))*(A(3, 5)*GDSF(2, I)+A(3, 6)*GDSF(1, I))
3)*CNST
C
55 CONTINUE
H(II+N3, JJ+N3)=H(II+N3, JJ+N3) + C1*SF(I)*SF(J)*CNST
H(II+N1, JJ+N1)=H(II+N1, JJ+N1) + C2*SF(I)*SF(J)*CNST
H(II+N2, JJ+N2)=H(II+N2, JJ+N2) + C2*SF(I)*SF(J)*CNST
60 JJ=NDF*J+1
70 II=NDF*I+1
80 CONTINUE
IF(NT.GT.1 .OR. IT.GT.1)GOTO 130
DO 110 NI=1, LGP
DO 110 NJ=1, LGP
XI=GAUSS(NI, LGP)
ETA=GAUSS(NJ, LGP)
CALL SHAPE (DET, ELXY, ETA, XI, NPE)
CNST=DET*WT(NI, LGP)*WT(NJ, LGP)
II=1
DO 100 I=1, NPE
JJ=1
DO 90 J=1, NPE
STIF(II+N3, JJ+N3)=STIF(II+N3, JJ+N3)+(GDSF(1, I)*(A45*GDSF(2, J)+A55*STI02070
1GDSF(1, J))+GDSF(2, I)*(A44*GDSF(2, J)+A45*GDSF(1, J)))*CNST
STIF(II+N3, JJ+N2)=STIF(II+N3, JJ+N2)+(A55*GDSF(1, I)*SF(J)+A45*GDSF(STI02090
12, I)*SF(J))*CNST

```

```

    STIF(I1+N2, JJ+N3)=STIF(I1+N2, JJ+N3)+(A55*GDSF(1, J)*SF(I)+A45*GDSF( ST102110
12, J)*SF(I))*CNST ST102120
    STIF(I1+N3, JJ+N1)=STIF(I1+N3, JJ+N1)+(A45*GDSF(1, I)*SF(J)+A44*GDSF( ST102130
12, I)*SF(J))*CNST ST102140
    STIF(I1+N1, JJ+N3)=STIF(I1+N1, JJ+N3)+(A45*GDSF(1, J)*SF(I)+A44*GDSF( ST102150
12, J)*SF(I))*CNST ST102160
    STIF(I1+N2, JJ+N2)=STIF(I1+N2, JJ+N2)+A55*SF(I)*SF(J)*CNST ST102170
    STIF(I1+N2, JJ+N1)=STIF(I1+N2, JJ+N1)+A45*SF(I)*SF(J)*CNST ST102180
    STIF(I1+N1, JJ+N2)=STIF(I1+N1, JJ+N2)+A45*SF(I)*SF(J)*CNST ST102190
    STIF(I1+N1, JJ+N1)=STIF(I1+N1, JJ+N1)+A44*SF(I)*SF(J)*CNST ST102200
90 JJ=NDF*J+1 ST102210
100 I1=NDF*I+1 ST102220
110 CONTINUE ST102230
    DO 120 I=1, NN ST102240
    DO 120 J=1, NN ST102250
    STFL(N, I, J)=STIF(I, J) ST102260
120 STIF(I, J)=0.0 ST102270
130 CONTINUE ST102280
    DO 140 I=1, NN ST102290
    DO 140 J=1, NN ST102300
140 STIF(I, J)=STIF(I, J)+STFL(N, I, J)+A0*H(I, J) ST102310
    DO 200 I=1, NN ST102320
    SUM=0.0 ST102330
    DO 180 K=1, NN ST102340
180 SUM=SUM+H(I, K)*(A0*W0(K)+A2*W1(K)+A3*W2(K)) ST102350
200 ELP(I)=ELP(I)+SUM ST102360
    RETURN ST102370
    END ST102380
    SUBROUTINE SHAPE (DET, ELXY, ETA, XI, NPE) SHA00010
C SHA00020
C ***** SHA00030
C SHA00040
C THIS SUBROUTINE EVALUATES THE SHAPE FUNCTIONS AND THEIR DERIVATIVES SHA00050
C AT THE GAUSSIAN POINTS (ISOPARAMETRIC QUADRILATERAL ELEMENT WITH SHA00060
C NINE NODES). SHA00070
C ***** SHA00080
C ***** SHA00090
C SHA00100
C IMPLICIT REAL*8 (A-H, O-Z) SHA00110
C DIMENSION ELXY(9, 2), XNODE(9, 2), NP(9), DSF(2, 9), GJ(2, 2), GJINV(2, 2) SHA00120
C COMMON/SHP/SF(9), GDSF(2, 9) SHA00130
C DATA XNODE/-1.000, 2*1.000, -1.000, 0.000, 1.000, 0.000, -1.000, 0.000, 2* SHA00140
1-1.000, 2*1.000, -1.000, 0.000, 1.000, 2*0.000/ SHA00150
C DATA NP/1, 2, 3, 4, 5, 7, 6, 8, 9/ SHA00160
C FNC(A, B)=A*B SHA00170
C IF (NPE-8) 50, 10, 70 SHA00180
10 DO 40 I=1, NPE SHA00190
    NI=NP(I) SHA00200
    XP=XNODE(NI, 1) SHA00210
    YP=XNODE(NI, 2) SHA00220
    XI0=1.0+XI*XP SHA00230
    ETA0=1.0+ETA*YP SHA00240
    XI1=1.0-XI*XI SHA00250
    ETA1=1.0-ETA*ETA SHA00260
    IF (I.GT.4) GO TO 20 SHA00270

```

	SF(NI)=0.25*FNC(XI0,ETA0)*(XI*XP+ETA*YP-1.0)	SHA00280
	DSF(1,NI)=0.25*FNC(ETA0,XP)*(2.0*XI*XP+ETA*YP)	SHA00290
	DSF(2,NI)=0.25*FNC(XI0,YP)*(2.0*ETA*YP+XI*XP)	SHA00300
	GO TO 40	SHA00310
20	IF (1.GT.6) GO TO 30	SHA00320
	SF(NI)=0.5*FNC(XI1,ETA0)	SHA00330
	DSF(1,NI)=-FNC(XI,ETA0)	SHA00340
	DSF(2,NI)=0.5*FNC(YP,XI1)	SHA00350
	GO TO 40	SHA00360
30	SF(NI)=0.5*FNC(ETA1,XI0)	SHA00370
	DSF(1,NI)=0.5*FNC(XP,ETA1)	SHA00380
	DSF(2,NI)=-FNC(ETA,XI0)	SHA00390
40	CONTINUE	SHA00400
	GO TO 120	SHA00410
50	CONTINUE	SHA00420
	DO 60 I=1,NPE	SHA00430
	XP=XNODE(I,1)	SHA00440
	YP=XNODE(I,2)	SHA00450
	XI0=1.0+XI*XP	SHA00460
	ETA0=1.0+ETA*YP	SHA00470
	SF(I)=0.25*FNC(XI0,ETA0)	SHA00480
	DSF(1,I)=0.25*FNC(XP,ETA0)	SHA00490
	DSF(2,I)=0.25*FNC(YP,XI0)	SHA00500
60	CONTINUE	SHA00510
	GO TO 120	SHA00520
70	DO 110 I=1,NPE	SHA00530
	NI=NP(I)	SHA00540
	XP=XNODE(NI,1)	SHA00550
	YP=XNODE(NI,2)	SHA00560
	XI0=1.0+XI*XP	SHA00570
	ETA0=1.0+ETA*YP	SHA00580
	XI1=1.0-XI*XI	SHA00590
	ETA1=1.0-ETA*ETA	SHA00600
	XI2=XP*XI	SHA00610
	ETA2=YP*ETA	SHA00620
	IF (1.GT.4) GO TO 80	SHA00630
	SF(NI)=0.25*FNC(XI0,ETA0)*XI2*ETA2	SHA00640
	DSF(1,NI)=0.25*XP*FNC(ETA2,ETA0)*(1.0+2.0*XI2)	SHA00650
	DSF(2,NI)=0.25*YP*FNC(XI2,XI0)*(1.0+2.0*ETA2)	SHA00660
	GO TO 110	SHA00670
80	IF (1.GT.6) GO TO 90	SHA00680
	SF(NI)=0.5*FNC(XI1,ETA0)*ETA2	SHA00690
	DSF(1,NI)=-XI*FNC(ETA2,ETA0)	SHA00700
	DSF(2,NI)=0.5*FNC(XI1,YP)*(1.0+2.0*ETA2)	SHA00710
	GO TO 110	SHA00720
90	IF (1.GT.8) GO TO 100	SHA00730
	SF(NI)=0.5*FNC(ETA1,XI0)*XI2	SHA00740
	DSF(2,NI)=-ETA*FNC(XI2,XI0)	SHA00750
	DSF(1,NI)=0.5*FNC(ETA1,XP)*(1.0+2.0*XI2)	SHA00760
	GO TO 110	SHA00770
100	SF(NI)=FNC(XI1,ETA1)	SHA00780
	DSF(1,NI)=-2.0*XI*ETA1	SHA00790
	DSF(2,NI)=-2.0*ETA*XI1	SHA00800
110	CONTINUE	SHA00810
120	DO 130 I=1,2	SHA00820


```

      IF(NPE .EQ. 4)GO TO 200
      NOD(1,5) = 2
      NOD(1,6) = NXX1 + (NPE-6)
      NOD(1,7) = NOD(1,3) - 1
      NOD(1,8) = NXX1+1
      IF (NPE .EQ. 9)NOD(1,9)=NXX1+2
200  IF(NY .EQ. 1)GOTO 225
      M = 1
      DO 220 N = 2,NY
      L = (N-1)*NX + 1
      DO 210 I = 1,NPE
210  NOD(L, I) = NOD(M, I)+NXX1+( IEL-1)*NEX1+KO*NX
220  M=L
225  IF(NX .EQ. 1)GO TO 255
      DO 250 NI = 2,NX
      DO 230 I = 1,NPE
      K1 = IEL
      IF(I .EQ. 6 .OR. I .EQ. 8)K1=1+KO
230  NOD(NI, I) = NOD(NI-1, I)+K1
      M = NI
      DO 250 NJ = 2,NY
      L = (NJ-1)*NX+NI
      DO 240 J = 1,NPE
240  NOD(L, J) = NOD(M, J)+NXX1+( IEL-1)*NEX1+KO*NX
250  M = L
C *****
C *****
C GENERATE THE COORDINATES X(I) AND Y(I)
C *****
C *****
255 DO 260 I=1, NXX1
260 DX(I) = XL/NXX
      DO 265 I=1,NYY1
265 DY(I) = YL/NYY
270 YC=0.0
      IF (NPE .EQ. 9) GOTO 300
      DO 290 NI = 1, NEY1
      I = (NXX1+( IEL-1)*NEX1)*(NI-1)+1
      J = (NI-1)*IEL+1
      X(I) = 0.0
      Y(I) = YC
      DO 275 NJ = 1,NXX
      I=I+1
      X(I) = X(I-1)+DX(NJ)
275 Y(I) = YC
      IF(NI .GT. NY .OR. IEL .EQ. 1)GO TO 300
      J = J+1
      YC = YC+DY(J-1)
      I = I+1
      X(I) = 0.0
      Y(I) = YC
      DO 280 II = 1, NX
      K = 2*II-1

```

```

MES00400
MES00410
MES00420
MES00430
MES00440
MES00450
MES00460
MES00470
MES00480
MES00490
MES00500
MES00510
MES00520
MES00530
MES00540
MES00550
MES00560
MES00570
MES00580
MES00590
MES00600
MES00610
MES00620
MES00630
MES00640
MES00650
MES00660
MES00670
MES00680
MES00690
MES00700
MES00710
MES00720
MES00730
MES00740
MES00750
MES00760
MES00770
MES00780
MES00790
MES00800
MES00810
MES00820
MES00830
MES00840
MES00850
MES00860
MES00870
MES00880
MES00890
MES00900
MES00910
MES00920
MES00930
MES00940

```

```

      I = I+1
      X(I) = X(I-1)+DX(K)+DX(K+1)
280  Y(I) = YC
290  YC = YC+DY(J)
      RETURN
C
300  DO 320 NI=1, NYY1
      I=NXX1*(NI-1)
      XC=0.0
      DO 310 NJ=1, NXX1
      I = I+1
      X(I) = XC
      Y(I) = YC
310  XC = XC + DX(NJ)
320  YC = YC + DY(NI)
      RETURN
      END
      SUBROUTINE BDUNSM(A, NRMAX, NCMAX, N, ITERM)
C *****
C EQUATION SOLVER FOR NON-SYMMETRIC SYSTEM OF
C EQUATIONS. SOLUTION IS STORED IN A(N,2*ITERM)
C *****
C IMPLICIT REAL*8(A-H,O-Z)
C DIMENSION A(NRMAX, NCMAX)
C CERO = 1.D-8
C PARE = CERO**2
C NBND=2*ITERM
C NBM = NBND - 1
C *****
C BEGINS ELIMINATION OF THE LOWER LEFT
C *****
C DO 1000 I=1, N
C IF (DABS(A(I, ITERM)) .LT. CERO) GO TO 410
C GO TO 430
410 IF (DABS(A(I, ITERM)) .LT. PARE) GO TO 1600
430 JLAST = MIN0(I+ITERM-1, N)
      L = ITERM + 1
      DO 500 J=I, JLAST
      L = L - 1
      IF (DABS(A(J, L)) .LT. PARE) GO TO 500
      B = A(J, L)
      DO 450 K=L, NBND
450  A(J, K) = A(J, K) / B
      IF (I .EQ. N) GO TO 1200
500 CONTINUE
      L=0
      JFIRST = I + 1
MES00950
MES00960
MES00970
MES00980
MES00990
MES01000
MES01010
MES01020
MES01030
MES01040
MES01050
MES01060
MES01070
MES01080
MES01090
MES01100
MES01110
BDU00010
BDU00020
BDU00030
BDU00040
BDU00050
BDU00060
BDU00070
BDU00080
BDU00090
BDU00100
BDU00110
BDU00120
BDU00130
BDU00140
BDU00150
BDU00160
BDU00170
BDU00180
BDU00190
BDU00200
BDU00210
BDU00220
BDU00230
BDU00240
BDU00250
BDU00260
BDU00270
BDU00280
BDU00290
BDU00300
BDU00310
BDU00320
BDU00330
BDU00340
BDU00350
BDU00360
BDU00370
BDU00380

```

```

      IF (JLAST .LE. 1) GO TO 1000
      DO 900 J= JFIRST, JLAST
      L=L+1
      IF (DABS(A(J, ITERM-L)) .LT. PARE) GO TO 900
      DO 600 K=ITERM, NBM
600  A(J, K-L) = A(J-L, K) - A(J, K-L)
      A(J, NBND) = A(J-L, NBND) - A(J, NBND)
      IF (1 .GE. N-ITERM+1) GO TO 900
      DO 800 K=1, L
800  A(J, NBND-K) = -A(J, NBND-K)
900  CONTINUE
1000 CONTINUE
1200 L = ITERM - 1
      DO 1500 I=2, N
      DO 1500 J=1, L
      IF (N+1-I+J .GT. N) GO TO 1500
      A(N+1-I, NBND) = A(N+1-I, NBND) - A(N+1-I+J, NBND)*A(N+1-I, ITERM+J)
1500 CONTINUE
      RETURN
1600 WRITE(6, 1601)
1601 FORMAT (' COMPUTATION STOPPED IN BNDEQ BECAUSE ZERO APPEARED ON
      1MAIN DIAGONAL. THE MATRIX FOLLOWS. ')
      WRITE(6, 1602) I, A(I, ITERM)
1602 FORMAT(10X, I5, E13.6)
      STOP
      END
      SUBROUTINE MATPRP (LAYER, C, A, H, THETA, AK, G13, G23, A44, A45, A55)
C
C *****
C
C SUBROUTINE MATPRP CALCULATES THE STANDARD COMPOSITE MATRICES QBAR
C (RELATES STRESS TO STRAINS FOR AN ARBITRARY ORIENTATION), AND
C THE A, B, AND D MATRICES WHICH RELATE THE STRESS AND MOMENT
C RESULTANTS TO THE STRAINS AND ROTATIONS.
C *****
C
      IMPLICIT REAL*8 (A-H, O-Z)
      COMMON /MAT/Q(16, 3, 3), Z(17), Q44(16), Q45(16), Q55(16)
      DIMENSION A(6, 6), C(3, 3), THETA(16), T(16)
      PI=3.14159265000
      DO 10 I=1, LAYER
10  T(I)=H/LAYER
      ZT=0.0
      LH=(LAYER-1)/2
      IF (LAYER/2*2.EQ. LAYER) LH=LAYER/2
      IF (LAYER/2*2.NE. LAYER) ZT=T(LH+1)*0.5
      IF (LAYER.EQ.1) GO TO 30
C
C *****
C
C CALCULATE THE Z'S, DISTANCES TO THE EDGES OF THE LAYERS FROM
C THE MIDPLANE
C *****

```

```

BDU00390
BDU00400
BDU00410
BDU00420
BDU00430
BDU00440
BDU00450
BDU00460
BDU00470
BDU00480
BDU00490
BDU00500
BDU00510
BDU00520
BDU00530
BDU00540
BDU00550
BDU00560
BDU00570
BDU00580
BDU00590
BDU00600
BDU00610
BDU00620
BDU00630
BDU00640
MAT00010
MAT00020
MAT00030
MAT00040
MAT00050
MAT00060
MAT00070
MAT00080
MAT00090
MAT00100
MAT00110
MAT00120
MAT00130
MAT00140
MAT00150
MAT00160
MAT00170
MAT00180
MAT00190
MAT00200
MAT00210
MAT00220
MAT00230
MAT00240
MAT00250
MAT00260
MAT00270
MAT00280
MAT00290

```

```

C
DO 20 I=1,LH
20 ZT=ZT+T(I)
30 Z(I)=-ZT
DO 40 I=1,LAYER
40 Z(I+1)=Z(I)+T(I)
WRITE(6,100)
WRITE(6,110) (T(I), I=1,LAYER)
WRITE(6,110) Z(I), (Z(I+1), I=1,LAYER)
WRITE(6,90)
DO 50 I=1,6
DO 50 J=1,6
50 A(I,J)=0.0
A55=0.0
A45=0.0
A44=0.0
DO 70 K=1,LAYER
C
*****
C
C READ IN THE ELEMENT PROPERTIES IF LAMINA ARE NOT IDENTICAL
C
C *****
C
C ANGLE=PI*THETA(K)/180.0
C CN=DCOS(ANGLE)
C SN=DSIN(ANGLE)
C
C *****
C
C CALCULATE THE QBAR MATRIX
C
C *****
C
Q(K,1,1)=C(1,1)*(CN**4)+2.0*(C(1,2)+2.0*C(3,3))*SN*SN*CN*CN+C(2,2)
1*(SN**4)
Q(K,1,2)=(C(1,1)+C(2,2)-4.0*C(3,3))*SN*SN*CN*CN+C(1,2)*(SN**4+CN**
14)
Q(K,2,2)=C(1,1)*(SN**4)+2.0*(C(1,2)+2.0*C(3,3))*SN*SN*CN*CN+C(2,2)
1*(CN**4)
Q(K,1,3)=(C(1,1)-C(1,2)-2.0*C(3,3))*SN*(CN**3)+(C(1,2)-C(2,2)+2.0*
1C(3,3))*(SN**3)*CN
Q(K,2,3)=(C(1,1)-C(1,2)-2.0*C(3,3))*(SN**3)*CN+(C(1,2)-C(2,2)+2.0*
1C(3,3))*SN*(CN**3)
Q(K,3,3)=(C(1,1)+C(2,2)-2.0*C(1,2)-2.0*C(3,3))*SN*SN*CN*CN+C(3,3)
1(SN**4+CN**4)
Q(K,2,1)=Q(K,1,2)
Q(K,3,1)=Q(K,1,3)
Q(K,3,2)=Q(K,2,3)
Q44(K)=G23*CN*CN+G13*SN*SN
Q45(K)=(G23-G13)*CN*SN
Q55(K)=G13*CN*CN+G23*SN*SN
C
*****
C
C *****

```

```

MAT00300
MAT00310
MAT00320
MAT00330
MAT00340
MAT00350
MAT00360
MAT00370
MAT00380
MAT00390
MAT00400
MAT00410
MAT00420
MAT00430
MAT00440
MAT00450
MAT00460
MAT00470
MAT00480
MAT00490
MAT00500
MAT00510
MAT00520
MAT00530
MAT00540
MAT00550
MAT00560
MAT00570
MAT00580
MAT00590
MAT00600
MAT00610
MAT00620
MAT00630
MAT00640
MAT00650
MAT00660
MAT00670
MAT00680
MAT00690
MAT00700
MAT00710
MAT00720
MAT00730
MAT00740
MAT00750
MAT00760
MAT00770
MAT00780
MAT00790
MAT00800
MAT00810
MAT00820
MAT00830
MAT00840

```



```

DUX=0.0
DUY=0.0
DVX=0.0
DVI=0.0
DWX=0.0
DWY=0.0
DSXY=0.0
DSYX=0.0
DSXX=0.0
DSYY=0.0
X=0.0
Y=0.0
DO 20 I=1,NPE
L=(I-1)*NDF+1
X=X+SF(I)*ELXY(I,1)
Y=Y+SF(I)*ELXY(I,2)
IF (NDF.LT.5) GO TO 10
DUX=DUX+GDSF(1,I)*W(L)
DUI=DUI+GDSF(2,I)*W(L)
DVX=DVX+GDSF(1,I)*W(L+1)
DVI=DVI+GDSF(2,I)*W(L+1)
10 DWX=DWX+GDSF(1,I)*W(L+N3)
DWI=DWI+GDSF(2,I)*W(L+N3)
SIX=SIX+SF(I)*W(L+N2)
SIY=SIY+SF(I)*W(L+N1)
DSXX=DSXX+GDSF(1,I)*W(L+N2)
DSXY=DSXY+GDSF(2,I)*W(L+N2)
DSYX=DSYX+GDSF(1,I)*W(L+N1)
20 DSYY=DSYY+GDSF(2,I)*W(L+N1)
IF(ITER .EQ. 1)GOTO 25
EX = DUX+0.5*DWX*DWX
EY = DVI+0.5*DWI*DWI
EXY=DUI+DVX+DWX*DWI
GOTO 26
25 EX = DUX
EY = DVI
EXY=DUI+DVX
26 DO 30 K=1,LAYER
SX=Q(K,1,1)*EX +Q(K,1,2)*EY +Q(K,1,3)*EXY
SY=Q(K,2,1)*EX +Q(K,2,2)*EY +Q(K,2,3)*EXY
TXY=Q(K,3,1)*EX +Q(K,3,2)*EY +Q(K,3,3)*EXY
SXZ=Q(K,1,1)*DSXX+Q(K,1,2)*DSYY+Q(K,1,3)*(DSXY+DSYX)
SYZ=Q(K,2,1)*DSXX+Q(K,2,2)*DSYY+Q(K,2,3)*(DSXY+DSYX)
TXYZ=Q(K,3,1)*DSXX+Q(K,3,2)*DSYY+Q(K,3,3)*(DSXY+DSYX)
TYZ=Q44(K)*(SIY+DWI)+Q45(K)*(SIX+DWX)
TXZ=Q45(K)*(SIY+DWI)+Q55(K)*(SIX+DWX)
SGMAXT=SX+Z(K)*SXZ
SGMAXB=SX+Z(K+1)*SXZ
SGMAYT=SY+Z(K)*SYZ
SGMAYB=SY+Z(K+1)*SYZ
SGMXYT=TXY+Z(K)*TXYZ
SGMXYB=TXY+Z(K+1)*TXYZ
IF(K .EQ. 1 .AND. NIJ .EQ. 1)STRSX=SGMAXT
STRXY=SGMXYT
30 CONTINUE
40 CONTINUE
RETURN
C
50 FORMAT (5X,10E12.4)
END

```

```

STRO0290
STRO0300
STRO0310
STRO0320
STRO0330
STRO0340
STRO0350
STRO0360
STRO0370
STRO0380
STRO0390
STRO0400
STRO0410
STRO0420
STRO0430
STRO0440
STRO0450
STRO0460
STRO0470
STRO0480
STRO0490
STRO0500
STRO0510
STRO0520
STRO0530
STRO0540
STRO0550
STRO0560
STRO0570
STRO0580
STRO0590
STRO0600
STRO0610
STRO0620
STRO0630
STRO0640
STRO0650
STRO0660
STRO0670
STRO0680
STRO0690
STRO0700
STRO0710
STRO0720
STRO0730
STRO0740
STRO0750
STRO0760
STRO0770
STRO0780
STRO0790
STRO0800
STRO0810
STRO0820
STRO0830
STRO0840
STRO0850
STRO0860
STRO0870
STRO0880

```

**The vita has been removed from
the scanned document**

TRANSIENT ANALYSIS OF LAYERED COMPOSITE PLATES ACCOUNTING
FOR TRANSVERSE SHEAR STRAINS AND VON KARMAN STRAINS

Daniel Joseph Mook

(ABSTRACT)

The increasing use of laminated composites in moving structures such as aircraft has led to a need for an efficient and accurate procedure for performing transient bending analysis of laminated composite plates. Classical theory is inadequate because it neglects transverse shear deformation, rotatory inertia, and geometric nonlinearities.

In this thesis, a theory to account for transverse shear deformation and rotatory inertia is combined with the von Karman theory of geometric nonlinearities to develop the nonlinear governing equations of laminated composite plate bending. A finite element program is developed to solve these equations, using the Newmark direct integration technique to integrate the equations in time. Apparently, this constitutes the first transient finite-element analysis of laminated composite plate bending which accounts for transverse shear deformation, rotatory inertia, and geometric nonlinearities. The program accuracy is verified by comparison with results previously reported in the literature. Finally, results of a study of various material and plate geometry parameters are presented.

The results of the parametric study show that transverse shear deformation, rotatory inertia, and geometric nonlinearity may all have a profound effect on the predicted bending response. In addition, the effects of material orthotropy, plate aspect ratio, plate thickness,

lamination scheme, and load magnitude are shown to be significant. Computational constants such as the Newmark coefficients, the time-step size, and the element mesh are also investigated, and appropriate observations are made on the computational aspects of the program.